1999

Petrology and geochemistry of late-stage intrusions of the A-type, mid-Proterozoic Pikes Peak batholith (Central Colorado, USA): implications for petrogenetic models

Diane R. Smith
Trinity University, dsmith@trinity.edu

J. Noblett

R. A. Wobus

D. Unruh

J Douglass
Trinity University

See next page for additional authors

Petrology and geochemistry of late-stage intrusions of the A-type, mid-Proterozoic Pikes Peak batholith (Central Colorado, USA): implications for petrogenetic models

D.R. Smith [a, *], J. Noblett [b], R.A. Wobus [c], D. Unruh [d], J. Douglass [a, 1], R. Beane [c, 2], C. Davis [e], S. Goldman [b], G. Kay [b], B. Gustavson [f], B. Saltoun [g], J. Stewart [h]

[a] *Department of Geosciences, Trinity University, 715 Stadium Drive, San Antonio TX 78212-7200, USA*

[b] *Department of Geology, Colorado College, Colorado Springs CO 80903, USA*

[c] *Department of Geology, Williams College, 947 Main Street, Williamstown MA 01267, USA*

[d] *U.S. Geological Survey, MS963, Box 25046, Federal Center, Denver CO 80225, USA*

[e] *Department of Geology, Washington & Lee University, Lexington VA 24450, USA*

[f] *Department of Geology, Carleton College, Northfield MN 55057, USA*

[g] *Department of Geology, College of Wooster, Wooster OH 44691-2363, USA*

[h] *Department of Geology, Beloit College, Beloit WI 53511, USA*

Abstract

The ~1.08 Ga anorogenic, A-type Pikes Peak batholith (Front Range, central Colorado) is dominated by coarse-grained, biotite ± amphibole syenogranites and minor monzogranites, collectively referred to as Pikes Peak granite (PPG). The batholith is also host to numerous small, late-stage plutons that have been subdivided into two groups (e.g. Wobus, 1976. Studies in Colorado Field Geology, Colorado School of Mines Professional Contributions, Colorado): (1) a sodic series (SiO_2 = ~44–78 wt%; K/Na = 0.32–1.36) composed of gabbro, diabase, syenite/quartz syenite and fayalite and sodic amphibole granite; and (2) a potassic series (SiO_2 = ~70–77 wt%; K/Na = 0.95–2.05), composed of biotite granite and minor quartz monzonite. Differences in major and trace element and Nd isotopic characteristics for the two series indicate different petrogenetic histories.

Potassic granites of the late-stage intrusions appear to represent crustal anatectic melts derived from tonalite sources, based on comparison of their major element compositions with experimental melt products. In addition, Nd isotopic characteristics of the potassic granites [ϵ_{Nd} (1.08 Ga) = −0.2 to −2.7] overlap with those for tonalites/granodiorites [ca 1.7 Ga Boulder Creek intrusions; ϵ_{Nd} (1.08 Ga) = −2.4 to −3.6] exposed in the region. Some of the partial melts evolved by fractionation dominated by feldspar.

The late-stage potassic granites share geochemical characteristics with most of the PPG, which is also interpreted to have an anatectic origin involving tonalitic crust. The origin of monzogranites associated with the PPG remains unclear, but mixing between granitic and mafic or intermediate magmas is a possibility.

* Corresponding author. Fax: +1-210-999-8264.
E-mail address: dsmith@trinity.edu (D.R. Smith)
1 Current address: Box 200, University of Rhode Island, Graduate School of Oceanography, Narrangansett, RI 02882, USA.
2 Current address: Department of Geology, 6800 College Station, Bowdoin College, Brunswick, ME 04011, USA.

Syenites and granites of the sodic series cannot be explained as crustal melts, but are interpreted as fractionation products of mantle-derived mafic magmas with minor crustal input. High temperature and low oxygen fugacity estimates (e.g. Frost et al., 1988. American Mineralogist 73, 727–740) support a basalt fractionation origin, as do ϵ_{Nd} values for sodic granitoids [ϵ_{Nd} (1.08 Ga) = +2.2 to −0.7], which are higher than ϵ_{Nd} values for Colorado crust at 1.08 Ga (ca −1.0 to −4.0). Enrichments in incompatible elements (e.g. rare earth elements, Rb, Y) and depletions in compatible elements (e.g. Cr, Sr, Ba) in the sodic granitoids compared to coeval mafic rocks are also consistent with fractionation. Accessory mineral fractionation, release of fluorine-rich volatiles and/or removal of pegmatitic fluids could have modified abundances of Ce, Nb, Zr and Y in some sodic granitoid magmas.

Gabbros and mafic dikes associated with the sodic granitoids have ϵ_{Nd} (1.08 Ga) of −3.0 to +3.5, which are lower than depleted mantle at 1.08 Ga, and their trace element characteristics suggest derivation from mantle sources that were previously affected by subduction-related processes. However, it is difficult to characterize the mantle component in these magmas, because assimilation of crust during magma ascent could also result in their observed geochemical features.

The Pikes Peak batholith is composed of at least two petrogenetically different granite types, both of which exhibit geochemical characteristics typical of A-type granites. Models proposed for the petrogenesis of the granitoids imply the existence of mafic rocks at depth and addition of juvenile material to the crust in central Colorado at ~1.1 Ga.

Keywords: A-type granites; Colorado; Geochemistry; Neodymium isotopes; Proterozoic

1. Introduction

The voluminous ~1.08 Ga Pikes Peak batholith occurs along the Front Range of central Colorado. The batholith is composed mostly of coarse-grained granite, but includes numerous late-stage intrusions with compositions ranging from gabbro to syenite to fayalite and sodic amphibole granite, as well as bodies of fine-grained granite (Fig. 1).

Previous studies (e.g. Anderson, 1983) interpreted the Pikes Peak batholith as an example of anorogenic granitic magmatism, based on the absence of internal deformation and contemporaneous tectonic boundaries. The Pikes Peak batholith is also one of the 'type examples' used by Loiselle and Wones (1979) in their definition of A-type granites. A-type granites have high Fe/(Fe+Mg) ratios and K_2O contents compared to S- and I-type granites, and probably crystallized from magmas characterized by low water and oxygen fugacities (Loiselle and Wones, 1979). Many models have been proposed for the origin of A-type granites, including fractionation of mantle-derived mafic magmas, with or without crustal assimilation (e.g. Loiselle and Wones, 1979; Barker et al., 1975, 1976; Foland and Allen, 1991; Turner et al., 1992; Kerr and Fryer, 1993), and partial melting of crustal materials (e.g. Anderson, 1983; Creaser et al., 1991; Collins et al., 1982; Whalen et al., 1987; Frost and Frost, 1997).

Barker et al. (1975), Hutchinson (1972, 1976), Wobus (1976), and Wobus and Anderson (1978) previously documented the field relations, petrography, mineralogy and major element chemistry of the batholith. Barker et al. (1976) published strontium, hydrogen and oxygen isotopic analyses of samples from the batholith. Based on their petrologic and geochemical studies, Barker et al. (1975, 1976) proposed a multi-stage model for the origin of the Pikes Peak batholith involving derivation of all the granitoids from mantle-derived basaltic magma that underwent 'reaction melting' with crust [i.e. assimilation-fractional crystallization (AFC) processes; cf Barker (1991)].

A single neodymium isotopic analysis (DePaolo, 1981a) of Pikes Peak granite (PPG) shows its composition to lie along the crustal evolution line for 1.8 Ga Colorado crust. DePaolo (1981a) interpreted the granite as the end product of a complex magmatic history of crystallization and crustal assimilation, beginning with a mantle-derived basaltic magma. Nd data for the observed spectrum of compositions, from gabbro to syenite and granodiorite to granite, were not documented, and thus limiting evaluation of petrogenetic models.

In this paper, we present new major and trace element and Nd isotopic data for rocks of late-stage plutons that comprise <10% (by areal exposure) of the Pikes Peak batholith (Fig. 1). Although small in area, the intrusions encompass a wide spectrum of lithologies from gabbro to intermediate and felsic compositions. In addition, we provide new geochemical data for coeval fine-grained dikes present in the Mount Rosa area (Gross and Heinrich, 1966; Goldman, 1993) and for samples of the main volume of granite comprising the batholith. Our results indicate that both fractionation of mantle-derived magmas and crustal anatexis were involved in the petrogenesis of magmas emplaced in the Pikes Peak batholith.

2. Regional geologic setting

The Pikes Peak batholith was emplaced ~1.08–1.09 Ga ago [U–Pb zircon dates; Schärer and Allègre (1982); Unruh, unpublished data] into rocks of the Colorado province of Bickford et al. (1986). This province, also referred to as the Yavapai province (Hoffman, 1988), represents addition of a >500 km-wide belt of rocks to the southern margin of the Archean Wyoming craton between 1790 and 1660 Ma (Reed et al., 1987). Crustal development involved the generation of volcanic–plutonic suites and associated greywacke–pelite facies that have been interpreted as relics of arc magmatism and related sedimentary basins developed along a convergent margin at the southern edge of the craton (Reed et al., 1987). These materials were consolidated during an episode of deformation, metamorphism and plutonism referred to as the Yavapai orogeny (Karlstrom and Bowring, 1987; additional references in Hoffman, 1988).

Wall rocks to the Pikes Peak batholith include metapelites and related metasediments that are intruded by the Boulder Creek and Silver Plume granitic batholiths (Wobus, 1976; Hutchinson, 1976; DePaolo, 1981a). Ages of the metamorphic rocks are not well defined, but accumulation and probably initial deformation and metamorphism, of shale and graywacke occurred before 1700 Ma ago (Bickford, 1988; Bickford et al., 1989); no pre-1800 Ma basement has been recognized (Reed et al., 1987). The metamorphic rocks are probably coeval with accretion of the Salida–Gunnison magmatic arc complex, interpreted to be a 1770 to 1730 Ma juvenile island arc terrane (Reed, 1987). Premo and Fanning (1997) provided new U–Pb zircon dates for two samples of the Boulder Creek batholith that establish the 'Boulder Creek plutonic event' at 1709.2 ± 3 Ma, which Premo and Fanning interpreted as related to the end of arc collision. The Silver Plume batholith is one of many anorogenic granitic plutons emplaced throughout Colorado 1420–1470 Ma ago (Bickford, 1988).

3. Geology and general petrology of the Pikes Peak batholith

The majority of the Pikes Peak batholith (>90% of areal exposure) is composed of biotite ± amphibole granites that are collectively called the PPG (e.g. Wobus and Anderson, 1978). Hutchinson (1960, 1972) mapped primary flow structures and fracture systems in the PPG and defined three structurally separate but texturally gradational intrusive centers, each ~20–25 km in diameter: the Buffalo Park; Lost Park; and Pikes Peak intrusive centers (Hutchinson, 1976; cf Fig. 1). Linear- and planar-flow structures and primary fracture systems within each intrusive center define a steeply inward-dipping, funnel-shaped pattern, indicating that magma rose at an angle of 65–80° along a S40–50° E direction (Hutchinson, 1976). The PPG is dominated by pink syenogranite (cf Hutchinson, 1960; Barker et al., 1975), but an arc-shaped body of distinctive gray monzogranite is found in the Buffalo Park intrusive center (Table 1).

However, it is the late-stage intrusions, comprising <10% of the exposed batholith, which led previous workers to hypothesize a complex, mantle-derived origin for the Pikes Peak batholith. Compositions of rocks from the late-stage intrusions define two chemical groups on the basis of alkali contents (Table 1; Wobus, 1976; Wobus and Anderson, 1978; Barker et al., 1975). The *potassic* series includes fine to medium biotite granites (and minor quartz monzonite) found in small stocks scattered throughout the batholith. They are collectively referred to and correlated with the Windy Point Granite of the Pikes Peak massif (Barker et al., 1975; see also Scott et al., 1978) and have been interpreted as late-stage, rapidly cooled variants of the PPG (Wobus, 1976). The fine-grained granites are resistant to weathering and erosion, and many of the topographically high portions of the batholith (e.g. the summit area of Pikes Peak, cf Fig. 1) are comprised of this unit (Wobus and Anderson, 1978).

Rocks of the *sodic* series are found in seven of the late-stage intrusions, including Sugarloaf, Tarryall, West Creek, Lake George, Spring Creek and Mount Rosa; an unnamed syenitic pluton is located in the Rampart Range near the eastern margin of the exposed batholith (Table 1; Fig. 1). Six of seven intrusions appear to lie along two NW–SE linears (Wobus, 1976). The plutons include a wide variety of rock types, from gabbro to syenite and granite, but no individual intrusion contains all of these rock types.

Gross and Heinrich (1966) reported the occurrence of ~50 widely scattered, dark gray dikes in the Mount Rosa area that they called lamprophyres. The dikes occur in association with both fine- and coarse-grained PPG as well as with Mount Rosa-type pegmatites (Gross and Heinrich, 1966; Goldman, 1993). They vary in width from <1 to ~8 m. Although some of the dikes are true camptonite lamprophyres (Goldman, 1993), stricter stipulations on the lamprophyre definition proposed by Rock (1991) eliminate

some of the dikes that Gross and Heinrich identified as lamprophyres; these latter dikes include quartz diorite, quartz monzonite and syenite (Goldman, 1993). Hornblende diabase dikes are also present (Goldman, 1993). For simplicity, here we refer to dikes with <53 wt SiO_2 as mafic dikes, and those with 53–65 wt% SiO_2 as intermediate dikes. These dikes exhibit geochemical features similar to those of the sodic series (see below), and thus are included here as part of that series.

4. Analytical techniques

Ninety samples representing both the sodic and potassic series were analyzed for their major and trace element compositions. Sample numbers beginning with 85, 86, 87, B65 and S71 were analyzed at the US Geological Survey for chemical data. Major elements and Rb, Ba, Sr, Y and Nb were determined by X-ray fluorescence (XRF) methods, Fe_2O_3 and FeO by titration methods (Reichen and Fahey, 1962), and Th and REEs by ICP methods.

Most of the other samples were analyzed for major elements and some trace elements by XRF methods at Franklin & Marshall College, Beloit College, Carleton College, Colorado College, or the University of Massachusetts-Amherst. Eight samples were analyzed for major and trace element contents by XRF methods at XRAL Activation Services, Inc. (Ann Arbor, MI, USA). For some samples, Fe_2O_3 and FeO contents were determined by iron titration after the method of Reichen and Fahey (1962). Trace element contents were determined by ICP methods at Franklin & Marshall, Beloit, and Carleton Colleges, and by neutron activation methods by XRAL Activation Services, Inc.

Because different laboratories were utilized for acquisition of major and trace element analyses, internal standards were routinely analyzed in order to check precision and accuracy. For elements determined by more than one method, the results by the most accurate method are reported. For major elements (Tables 2–10) average estimated errors (% of amount present) are 1–2% for SiO_2, Al_2O_3, Fe_2O_3 and K_2O; 5% for TiO_2, CaO, Na_2O and P_2O_5; and between 5 and 15% for MnO and MgO (because MgO is in such low concentrations in some rocks). Except for Ni, Zn, Nb and Ga, average estimated errors for trace element analyses range between 3 and 10%. Errors are ~10% for Ni, Zn and Nb, and ~20% for Ga.

Of all the samples analyzed for major and trace elements, 32 were selected for Nd isotopic analysis (Table 11). Sample numbers beginning with 85, 86, 87, B65 and S71 were analyzed at the US Geological Survey, and the other samples were analyzed at Rice University. Nd and Sm contents and isotopic ratios were determined by isotope dilution and mass spectrometric methods (see Table 11 for details).

5. Intensive parameters

Fayalite, hedenbergite, annite-rich biotite and sodic and iron-rich amphiboles have been documented in Pikes Peak sodic granitoids (Barker et al., 1975; Giambalvo, 1993). The anhydrous and iron-rich nature of late-crystallized ferromagnesian minerals in the sodic granitoids reflects crystallization from relatively dry and reduced magmas, which is typical for A-type, anorogenic granites (Loiselle and Wones, 1979; Anderson, 1983). For sodic series syenites and fayalite granites, oxygen fugacities have been estimated at or below (≤ ~1.5 log units) the quartz–fayalite–mag-netite buffer (Barker et al., 1975; Frost et al., 1988). In addition, melt temperatures probably exceeded 950°C for the sodic granitoids. Frost et al. (1988) estimated temperatures in the range of 970 to 650°C, although the lower end of the range may reflect subsolidus re-equilibration. Saltoun (1993) estimated zircon saturation temperatures (Watson and Harrison, 1983) for Mount Rosa fayalite granite that range from 966 to 865°C. Beane (1993) estimated apatite saturation temperatures (Harrison and Watson, 1984) for Sugarloaf syenites that range from 961 to 724°C.

A few estimates of intensive parameters have been made for Pikes Peak potassic series granites. Barker et al. (1975) showed that granites of the main PPG do not plot along minimum melt compositions of water-saturated granites in the normative quartz–albite–orthoclase ternary. Potassic granites of the main PPG and the Windy Point-type granites instead plot towards the Or apex, suggesting crystallization under conditions of low water activity ($P_{H_20} < P_{total}$; Fig. 2). Pikes Peak potassic granites have petrologic and geochemical characteristics similar to those of the Watergums granite of the Lachlan fold belt in Australia (Clemens et al., 1986; cf Fig. 2), which was inferred to have water contents ranging from 2.4 to 4.3 wt% (Clemens et al., 1986). Granitic magmas of the Pikes Peak batholith probably were not water-saturated until very late in their crystallization history, but magmatic fluorine abundances may have been relatively high. Fluorite is a common accessory mineral and fluorine abundances range from <0.1 to ~0.7 wt% in rocks of both the sodic and potassic series (Barker et al., 1975). The relatively high temperatures and low water contents estimated for Pikes Peak magmas are consistent with shallow emplacement at depths of <5 km (Barker et al., 1975).

6. Major and trace element chemistry

Tables 2–10 give major and trace element compositions of rocks of the sodic and potassic series and the data are presented graphically in Figs. 3–7.

Most mafic rocks of the sodic plutons include Fe-enriched alkaline to subalkaline gabbro and mafic dikes. The exception is sample CCN-19-CD, which has high MgO (11.5 wt%) and compatible element abundances (Co=65 ppm; Ni=280 ppm; Cr=650 ppm) that suggest it is a cumulate rock. For the gabbros and mafic dikes, wide variations are observed in many elements [e.g. Na_2O, K_2O, TiO_2, MnO, P_2O_5, rare earth elements (REE), Rb, Th, U, Nb, P, Ti and Cs; cf Tables 2 and 3 and Figs. 3, 5 and 6]. Many element abundances and ratios do not systematically vary with silica (or MgO) (cf Figs. 3 and 4), but instead exhibit considerable scatter. Primitive mantle-normalized incompatible element patterns for mafic dikes and gabbros are shown in Fig. 6. The patterns exhibit overall enrichments, but have 'troughs' at Nb, Ta and Sr. Th depletions and Rb enrichments are also observed in patterns for a mafic dike.

Most of the sodic granitoids are metaluminous to peraluminous, but some of the sodic amphibole granites and most of the syenites are peralkaline. Granites of the late-stage potassic intrusions (Windy Point-type granites) are peraluminous to metaluminous in composition. The Windy Point-type granites are chemically similar to the coarse-grained pink PPG that comprises the bulk of the batholith (cf Figs. 3–5). When the late-stage potassic granites plus the pink PPG are compared with the gray monzogranites, most major and trace element characteristics are found to overlap. However, the gray monzogranites trend towards lower silica and REE and higher Ba, Sr, Eu, Cr, V, Sc and Co contents [cf Figs. 3, 5 and 7 (b) and Tables 8–10].

Granitoids of both the potassic and sodic series exhibit geochemical features typical of A-type granites (e.g. Whalen et al., 1987), including low Mg-numbers (molar Mg/[Mg+Fe]×100), high K_2O/MgO, low abundances of Sr, Eu, Sc, V, Ni, Cr and Co, and high abundances of Rb, Ba, Zr, Y, Nb, La, Ce, Ga and F compared to S- and I-type granites. A-type granites often occur in bimodal association with mafic rocks (e.g. Turner et al., 1992) but granites of the Pikes Peak batholith are found in association with intermediate compositions, as well as gabbros and mafic dikes (cf Fig. 3). Granitoids of the potassic and sodic series with up to ~70 wt% SiO_2 can be distinguished on the basis of abundances and ratios of some major and minor elements (e.g. Na_2O, TiO_2, CaO, P_2O_5, Mg-number; cf Figs. 3 and 4). Trends of Rb/Sr and Y/Sc with SiO_2 also serve to distinguish between the potassic and sodic series for rocks with up to ~72 wt% SiO_2 (Fig. 4), but many trace element abundances and ratios exhibit overlap between the two series (cf Figs. 5 and 7).

7. Isotopic geochemistry

Table 11 gives new Sm–Nd data for samples of the Pikes Peak batholith. Age data are not available for all 32 samples that have been analyzed. Unruh (unpublished data) has obtained U–Pb zircon dates for three samples of PPG of the main phase of the batholith that range from 1072 to 1090 Ma. Unruh also has U–Pb zircon data for the late-stage intrusions ranging from 1070 to 1090 Ma for the potassic series and from ~1080 to 1090 for the sodic series, but associated errors on some dates (especially the younger dates) do not allow distinction among these dates. The U–Pb dates are somewhat older than Rb–Sr and K–Ar dates for the batholith previously compiled by Hutchinson (1976), which give an average of ~1.03 Ga.

To simplify presentation and discussion of the Nd isotopic data, we refer to $\epsilon_{Nd}(T)$ values calculated at T=1.08 Ga for all samples. Fig. 8 shows our neodymium data plotted versus silica, and Fig. 9 shows our neodymium isotopic data plotted versus age. Also illustrated in Figs. 8 and 9 are currently available data (shown as fields) for wall rocks and mantle (DePaolo, 1981a). Although there is overlap between the ranges in $\epsilon_{Nd}(T)$ for sodic and potassic series rocks, the range for sodic syenites and granites (+2.2 to −0.7) extends to higher values than the range for potassic series granites (−0.2 to −2.7). Sodic series syenites and granites lie above the Colorado crustal evolution line at 1.08 Ga, whereas the potassic rocks lie either within or just slightly above it (Fig. 9).

8. Discussion

8.1. Mafic rocks and mantle source characteristics

$\epsilon_{Nd}(T)$ values for two samples of a mafic dike from Mount Rosa are identical (+3.5) and the highest of all samples analyzed here. $\epsilon_{Nd}(T)$ values for four of the five analyzed gabbros range from +0.4 to +1.9, plotting between estimates for depleted mantle and ~1.4–1.8 Ga crustal wall rocks [DePaolo, 1981a; Figs. 8 and 9(a)]. The fifth gabbro has $\epsilon_{Nd}(T)$ of −3.0, which lies within the range for ~1.8 Ga Colorado crust; this is also the gabbro with the highest Mg-number and compatible element concentrations among the Pikes Peak mafic rocks analyzed here.

Few Sr and O isotopic analyses exist for Pikes Peak mafic rocks, but the available data (Barker et al., 1976) support their mantle-derived origin. Compared to the relatively limited range for intermediate and

felsic rocks, the mafic rocks exhibit a large range in $\epsilon_{Nd}(T)$ values [Figs. 8 and 9 (a)], from +3.5 to −3.0. Although many mantle reservoir types have been proposed (e.g. see Table 6.5 of Rollinson, 1993), we take a simple approach here and consider three possible mantle sources:

1. 'depleted' mantle;
2. 'enriched' mantle; and
3. supra-subduction zone (SSZ) mantle.

'Depleted' mantle sources have geochemical characteristics that upon partial melting generally result in mid-ocean ridge basalts (MORB) with smooth, primitive mantle-normalized trace element patterns with no 'anomalies' and progressive depletions in the more incompatible elements [Fig. 6 (c); cf Pearce (1983)]. Assuming DePaolo's (1981a) ϵ_{Nd} evolution line for depleted mantle, the predicted $\epsilon_{Nd}(T)$ at 1.08 Ga would be ca +6.0. Upon partial melting, 'enriched' mantle sources yield basalts similar to ocean island basalts (OIB); that is, they exhibit enrichments in incompatible trace elements [cf Fig. 6 (c)], with relative enrichment of Nb and Ta compared to the light REE (LREE) and large ion lithophile elements [LILE; e.g. Rb, K; Weaver (1991)]. Initial Nd isotopic ratios would be less radiogenic than depleted mantle, including negative $\epsilon_{Nd}(T)$ values within the range exhibited for continental crust (e.g. Hawkesworth and Vollmer, 1979). SSZ mantle sources are fossil mantle wedges above subduction zones that were metasomatized by LILE-rich and/or LREE-rich fluids and/or melts derived from the subducted slab (e.g. Tatsumi et al., 1986; Jenner et al., 1987; Hergt et al., 1991; Hawkesworth et al., 1991). Although this source is a complex region of hybridization and metasomatism (e.g. Wyllie, 1984), basaltic melts derived from it would generally be characterized by primitive mantle-normalized trace element patterns enriched in incompatible elements but with negative Nb (and Ta) anomalies (e.g. Pearce, 1983; Davidson, 1996; cf Fig. 6). $\epsilon_{Nd}(T)$ values are not easily predicted, but would be expected to lie below the depleted mantle evolution curve.

Trace element patterns (Fig. 6) and Nd isotopic characteristics of Pikes Peak mafic rocks are consistent with their derivation from an SSZ mantle source. Perhaps SSZ mantle was accreted to the continental lithosphere as a result of collision of the Salida–Gunnison arc terrane at ~1.7 Ga, and was a source for magmatism commencing at 1.08 Ga. Subduction-related metasomatism could have resulted in veins that were enriched in fluid-soluble trace elements (e.g. Ba, Rb, Th, K, Sr; cf Tatsumi et al., 1986) and had relatively low melting temperatures compared with their mantle host (Huppert and Sparks, 1985). Upon melting of this heterogeneous source, mafic magmas with variable $\epsilon_{Nd}(T)$ and Nb-depleted trace element patterns would be expected. Even if SSZ mantle was not the direct source material for Pikes Peak mafic magmas, magmas generated from other, presumably 'enriched' sources could have selectively assimilated

metasomatic veins as they traversed the upper mantle (cf Huppert and Sparks, 1985), resulting in 'arc-type' geochemical signatures.

However, crustal assimilation during magma ascent has also been suggested to cause negative Nb anomalies in some basaltic rocks (e.g. Thompson et al., 1982; Campbell and Griffths, 1990; Pearce, 1983). In simple crustal assimilation models, the size of Nb–Ta anomalies and concentrations of elements most affected by contamination (Ba, Rb, K, LREE, Sr; Thompson et al., 1982) are expected to increase with progressively more negative $\epsilon_{Nd}(T)$ values. These relationships are not observed among Pikes Peak mafic rocks. For example, K_2O contents generally decrease with lower $\epsilon_{Nd}(T)$, and the two samples with the lowest and the highest $\epsilon_{Nd}(T)$ values (−3.0 and +3.5) have comparable La/Nb ratios (i.e. the size of the Nb anomalies is similar). Barnes et al. (1999) emphasized that assimilation of crustal rocks into a primitive basaltic magma will be accompanied by fractional crystallization (FC) and that Nb will not be depleted unless a significant amount of an oxide phase (s), with a large distribution coefficient for Nb, is included in the fractionating assemblage. High abundances of Fe and Ti (cf Tables 2 and 3) in Pikes Peak mafic rocks indicate that oxide minerals (e.g. magnetite, ilmenite) were not removed from parental magmas. Hence, the Nb depletions in these rocks are difficult to explain by AFC processes (cf Barnes et al., 1999).

In summary, mafic rocks of the Pikes Peak batholith exhibit primitive-normalized trace element patterns with Nb–Ta depletions and a considerable range in $\epsilon_{Nd}(T)$. These geochemical features are consistent with derivation of mafic magmas from heterogeneous SSZ mantle sources, but it is difficult to dismiss contamination of mantle-derived magmas during ascent through the overlying crust.

8.2. Petrogenetic models for intermediate and felsic magmas

Rocks of the sodic and potassic series can be distinguished on the basis of associated rock types, ferromagnesian mineralogy and selected major and trace element abundances and ratios (Wobus, 1976; Wobus and Anderson, 1978). Ranges in Nd isotopic ratios are slightly different for the two series, and the petrologic and geochemical differences suggest different petrogeneses.

Barker et al. (1975, 1976) developed a 'reaction melting' model to explain the origin of the Pikes Peak batholith. They proposed that mantle-derived basaltic magmas were ultimately the parents from which Pikes Peak intermediate and felsic magmas were derived. Reaction melting (i.e. AFC) involved basalts

and lower crust that was already depleted in K_2O due to generation of large volumes of granitic magmas during the ~1.7 Ga Boulder Creek event and the ~1.4 Ga Silver Plume event. This resulted in generation of syenitic magmas, the bulk of which underwent further reaction with intermediate crust to produce the voluminous potassic granites. They also suggested that some basaltic magmas directly interacted with granitic crust to produce the potassic granites. Some of the syenitic magmas underwent fractionation (possibly accompanied by assimilation) to produce the sodic granites emplaced in the seven late-stage intrusions.

Our geochemical data are consistent with some aspects of the model proposed by Barker et al. (1975), namely that sodic series magmas were the result of extensive fractionation of mantle-derived mafic magmas, and that intermediate crust was involved in the origin of the potassic magmas. However, for the potassic granites, the data are also consistent with a direct origin from the crust via partial melting, rather than derivation from mantle-derived magmas by AFC processes.

8.2.1. Crustal partial melting models

Since Barker et al. (1975) proposed their model, additional models have been developed for the origin of A-type granites. Many of these invoke partial melting of crustal sources of various lithologies, including residual or restitic lower crust (e.g. Collins et al., 1982; Whalen et al., 1987), underplated basalts and their differentiates (Frost and Frost, 1997), and tonalite/granodiorite (e.g. Anderson, 1983; Sylvester, 1989; Creaser et al., 1991).

Residual source models call upon materials left after a previous event of melt generation and extraction (e.g. Collins et al., 1982; Clemens et al., 1986; Whalen et al., 1987). The ~1.7 Ga Boulder Creek granodiorites are the products of the first voluminous magmatic episode in central Colorado and they could represent crustal melts [cf Fig. 9 (a)]. In addition, the ~1.4 Ga Silver Plume-type intrusions have also been interpreted as representing melts from crustal sources (e.g. Anderson and Morrison, 1992). Perhaps the residual materials left after one or both of these previous magmatic episodes were remelted to generate granitic magmas emplaced in the Pikes Peak batholith. ϵ_{Nd} ratios for the Silver Plume rocks at 1.08 Ga are less radiogenic than those for Pikes Peak granitoids (Fig. 8), ruling out a common source for these two intrusive suites. Also, as is the case for many A-type granites, the high incompatible to compatible element ratios, high iron to magnesium ratios and high potassium contents in Pikes Peak granitoids argue against their derivation from highly LILE-depleted sources (e.g. Sylvester, 1989; Creaser et al., 1991). Unless the source has undergone secondary enrichment, only very low degrees of melting of

residual sources can explain these geochemical features. Melt segregation and extraction are difficult (to impossible) to envisage at extremely low degrees of melting (McKenzie, 1985; Wickham, 1987), especially for the large amounts of granite found in the batholith.

Frost and Frost (1997) emphasized the extreme iron enrichment and reduced nature of anorogenic 'rapakivi' granites (including the Pikes Peak batholith) and proposed that mantle-derived, tholeiitic basalts that underplate the crust and undergo differentiation might, in turn, experience modest degrees of partial melting to produce granitic magmas. However, Roberts and Clemens (1993) emphasized the unsuitability of basaltic lithologies as potential sources for potassic granites. Fig. 10 illustrates major element abundances in melts experimentally generated from mafic sources (e.g. Helz, 1976; Beard and Lofgren, 1991). These melts do not have the K_2O, Na_2O and/or CaO contents observed in the sodic series granitoids, nor are they good matches for the potassic granites. Fig. 10 also illustrates a melt generated from ferrodiorite (Scoates et al., 1996; Mitchell et al., 1996), which is depleted in Na_2O compared to the sodic granitoids. Furthermore, the severe depletions of Ba and Sr in many of the sodic granitoids, as well as the trends in these elements among the sodic rocks, are not observed in magmas derived by variable degrees of melting of either ferrodiorite or mafic source rocks [Fig. 7 (b)].

Partial melting of a tonalite/granodiorite source appears to be a viable model for the potassic series granites. Fig. 11 illustrates major element compositions of Pikes Peak potassic rocks and compositions of experimentally produced melts from tonalite/granodiorite sources (e.g. Skjerlie and Johnston; 1993; Patiño Douce, 1997). Good matches between the compositions of many Pikes Peak potassic granites and the experimentally produced melts lend support to a crustal anatectic origin, but we emphasize that the melt compositions are composition and pressure dependent [e.g. Figs. 11 (e and f)]. Wall rocks of the Pikes Peak batholith include extensive granodiorite and tonalite plutons of the Boulder Creek intrusive period (ca 1.7 Ga) with major element compositions similar to those used in the melting experiments (cf Gable, 1980) and ϵ_{Nd} (1.08 Ga) values that overlap with those for the potassic granites (Fig. 8). However, it is probable that exposed wall rocks and the currently available Nd isotopic data for wall rocks may not accurately represent basement lithologies. Unexposed, deeper tonalites could be characterized by higher Sm/Nd than presently exposed Boulder Creek rocks, thus evolving to higher $^{143}Nd/^{144}Nd$ at 1.08 Ga and eliminating the apparent need for a more juvenile component in some of the potassic granites that lie above the crustal evolution line in Fig. 9(c).

Some of the potassic granites exhibit lower Ba and Sr contents than expected for melts from tonalitic sources [Fig. 7 (b)]. However, these characteristics can be explained by further evolution of crust-derived

magmas due to crystal fractionation dominated by feldspar, and perhaps involving accessory minerals [cf Figs. 5 (f) and 7 (b)]; also see Section 8.2.3).

As noted above, potassic granites of the late- stage intrusions are geochemically comparable to the pink PPG. A crustal anatectic origin also seems plausible for the pink PPG, especially in view of the immense exposure of this material (>3000 km2, cf Fig. 1). Major element composi- tions of the pink PPG overlap with those for melts mafic produced in experiments involving tonalite sources (Fig. 11), and their Nd isotopic characteristics are also consistent with a crustal origin [cf Fig. 9 (c)].

However, the gray monzogranites (and sample 86TQM) exhibit lower silica contents and trends that diverge from those for melts derived by fluid-absent melting of tonalite (Fig. 11). Perhaps anatexis involved higher degrees of melting than was achieved in those experiments (up to ~40%), but without experimental confirmation of the compositions of such melts, it is difficult to evaluate this possibility. Hydrous melting of tonalite produces melts with SiO_2, CaO and MgO contents similar to those in the monzogranites, but such melts also contain higher Na_2O and Al_2O_3 and lower K_2O, FeO^T and TiO_2 (cf Carroll and Wyllie, 1990). Nor can mixing between melts from these two sources ('wet' and 'dry' tonalites) explain the major element characteristics of the gray monzogranites. Mafic source rocks seem to be required, and dehydration experiments involving metabasaltic sources (e.g. Rushmer, 1991) have resulted in intermediate compositions. The melts are not as alkalic as the monzogranites (Fig. 10), but the alkali content of the melt will be sensitive to the starting material (Beard and Lofgren, 1991). It is difficult to further assess this alternative because there are few data from experiments involving alkaline basalt sources. Another possible source lithology is ferrodiorite, which Frost and Frost (1997) proposed as a potential source for anorogenic granites, but the limited experimental data that exist (Scoates et al., 1996) indicate that melt derived from ferrodiorite is not siliceous enough to be a good match for the gray monzogranites (Figs. 10 and 11).

In contrast to the case for the potassic series granites, partial melting of tonalitic/granodioritic crust does not explain the observed major element variations for the sodic series granitoids. Melts from these sources are depleted in Na_2O and enriched in MgO (and CaO) compared to the sodic granitoids (Fig. 11). Furthermore, low oxygen fugacities estimated for the sodic magmas severely limit the amount of crust in those magmas (Frost and Frost, 1997). Trace element characteristics of the sodic syenites and granites also argue against an origin by partial melting of crust. Depletions in Ba and Sr in many of the sodic granitoids can not be explained by partial melting of tonalite sources [Fig. 7 (a)]. In addition, high Rb/Sr ratios (>10) characterize most of the sodic syenites and granites [Fig. 4 (b)]. For example, Rb/Sr ranges

from 16 to 57 in the sodic amphibole granites. Halliday et al. (1991) showed that Rb/Sr values > ~5–10 cannot be attained by partial melting involving crustal rocks, but rather are the result of crystal fractionation. Lastly, the sodic granitoids do not have Nd isotopic characteristics similar to those for Colorado crust at 1.08 Ga [Figs. 8 and 9(b)].

In summary, crustal anatexis involving tonalite appears to be a viable petrogenetic model for the late-stage potassic intrusions and possibly the pink PPG. In contrast, the major and trace element and Nd isotopic characteristics of the sodic series syenites and granites are inconsistent with an origin by partial melting of any known crustal lithologies.

8.2.2. Crystal fractionation models and the sodic series

A viable model for the sodic series syenites and granites involves extreme fractionation of basaltic melts. Characteristics of this series that support a basalt fractionation origin include a range of compositions from gabbro and diabase to syenite and granite, the relatively small volumes of these magma types emplaced in the batholith (they represent <3% of the total exposed area), and estimates of low oxygen fugacities and relatively high temperatures during crystallization of sodic granitoid magmas. Depletions in compatible elements (e.g. Ni, Cr, Co, Ba, Sr, Eu, Ti) and enrichments in incompatible elements (e.g. REE, Nb, Y, etc.) compared to coeval mafic rocks (cf Fig. 12) suggest prolonged fractionation involving feldspar and ferromagnesian phases (e.g. olivine, pyroxene) from parental basalts. Magmas parental to sodic syenites and granites are inferred to be largely mantle-derived because ϵ_{Nd} values for the syenites and granites are higher than those expected for most crustal lithologies exposed in the region [Figs. 8 and 9 (b)].

Figs. 13 and 14 illustrate ocean island suites for which crystal fractionation of basaltic magmas has been invoked as the dominant process generating intermediate and felsic rocks (Harris, 1983; LeRoex, 1985; Macdonald et al., 1990). Also illustrated in Fig. 13 are several granite compositions that have been interpreted as the result of prolonged fractionation of coeval mafic intrusive rocks [samples 3, 5, 8 and 10 of Table 2 in Turner et al. (1992)]. These granitic differentiates have major element compositions that are very similar to those of the Pikes Peak sodic granites. Likewise, generally good matches are found between the sodic Pikes Peak and ocean island suites, lending support to a fractionation model. However, no single line of descent characterizes the Pikes Peak sodic suite, suggesting removal of assemblages composed of different mineral proportions.

Trace element trends and abundances in Pikes Peak sodic rocks also support a fractionation model. Depletions in Cr (and Ni, V, etc., not illustrated) with decreasing MgO [Fig. 14 (a)] suggest removal of olivine and/or pyroxene early in the fractionation history. Progressively larger Eu anomalies and Sr depletions with increasing differentiation [Figs. 5 and 14 (c)] indicate the separation of plagioclase, and large depletions in Ba (and Sr) suggest an important role for potassium feldspar fractionation later in the fractionation history [Figs. 7 (a) and 15]. As previously noted, high Rb/Sr ratios for most sodic syenites and granites [Fig. 4 (b)] are probably the result of fractionation (versus partial melting) processes (cf Halliday et al., 1991).

Rare earth and high field strength elements (HSFE) are generally less mobile during weathering and/or hydrothermal alteration than are Ba, Sr and Rb. However, they will be very sensitive to fractionation of even small amounts of accessory minerals (e.g. zircon, allanite, sphene, Fe–Ti oxides). Scatter and depletions in Ce, Nb, Y and Zr in Pikes Peak sodic rocks compared to ocean island suites [Figs. 14 (e–h)] could reflect removal/accumulation of only small amounts of accessory minerals, whereas the ocean island suites may not have been strongly influenced by accessory mineral fractionation.

Another process that could have affected the abundances of REE and HFSE (and Th) includes formation of residual pegmatitic fluids. Simmons et al. (1987) documented the geochemistry of pegmatites and associated host rocks in the northern portion of the batholith. They found that variations in many major and trace elements in the PPG, monzogranite (called quartz monzonite by Simmons et al.) and pegmatite wall zones can be explained by diffusive differentiation and FC. But their investigations also showed that REE, Y, Zr and Th were strongly partitioned out of the pegmatite wall zones into residual pegmatitic fluids. Although Simmons et al. (1987) studied rocks of the potassic series, perhaps pegmatitic fluids removed these elements (and possibly Nb) from some sodic syenitic and granitic magmas. Pegmatites are found in association with several of the sodic plutons (e.g. Mount Rosa, Lake George), and evolution of pegmatitic fluids could explain incoherent trends for some elements in the sodic series compared to the ocean island suites (cf Fig. 14), and depletions in HFSE in some syenites and the sodic amphibole granites relative to Pikes Peak mafic rocks (cf Fig. 12). Another possibility includes the release of magmatic volatiles, particularly if fluorine was in high concentrations. Charoy and Raimbault (1994) proposed that a F-rich fluid phase developed late in the crystallization history of an A-type granitic magma in China and that HFSE, as fluorinated complexes, were efficiently partitioned into that fluid (cf Webster and Holloway, 1990).

For the Pikes Peak sodic series, there is significant scatter in plots of $\epsilon_{Nd}(T)$ and 1/Nd (Fig. 15),

suggesting either a complex petrogenesis or perhaps even precluding AFC. AFC models involving wall rocks of the batholith (Boulder Creek and Silver Plume intrusions) show that only minor assimilation of these materials is allowed because fairly high rates of assimilation generally cannot produce the high Nd concentrations in some of the sodic granitoids [Fig. 15(a)]. Crustal input is also limited by low oxygen fugacities estimated for sodic granitoid magmas. Parental basalts with $\epsilon_{Nd}(T)$ inherited from SSZ mantle sources could have evolved into sodic syenitic and granitic magmas by FC with little or no crustal involvement [cf Fig. 15 (b)].

Uncertainty with any fractionation model proposed for the Pikes Peak sodic series involves the nature of parental mafic magmas. Nearly all Pikes Peak mafic rocks exhibit geochemical features (low Mg-numbers, depletions in compatible elements such as Cr and Ni) that indicate significant fractionation prior to emplacement. It is thus difficult to assess the nature of primary mafic magmas that were parental to Pikes Peak sodic syenites and granites because the former are likely not represented by the sampled gabbros and diabase dikes. Notwithstanding uncertainties regarding parental magma compositions and the isotopic nature of the mantle source(s), we propose that the petrologic and geochemical characteristics of the sodic syenites and granites are supportive of a mantle- derived, fractionation origin.

8.2.3. Crystal fractionation models and the potassic series

The petrogenetic model for the potassic granites proposed by Barker et al. (1975) calls upon evolution of basaltic and/or syenitic magmas by FC and assimilation of granitic crust. Simmons et al. (1987) also called upon FC in the evolution of monzogranitic magmas to generate the PPG. Trends on many geochemical plots (e.g. Figs. 3, 4 and 7) generally support a relationship among the gray monzogranites, pink PPG and Windy Point-type granites by FC processes. However, the syenites do not appear to represent magmas parental to the potassic granitoids. They clearly cannot be parental to the gray monzogranites because they overlap in silica contents but show distinctions in most other elements and ratios (cf Figs. 3 and 4). Distinct trends in Rb/Sr versus silica between the syenites and the potassic granitoids also preclude a relationship between these two groups by FC [Fig. 4 (b)]. It is also difficult to relate Pikes Peak mafic rocks as parental magmas to the potassic granitoids. For example, Rb/Sr values project from the potassic granitoids back to the gabbros, but the mafic dikes do not appear to be plausible parents to potassic series granitoids [Fig. 4 (b)]. Between the gabbros and monzogranites, trends in Mg-number and Na_2O with increasing silica [Figs. 4 (a) and 10 (b)] are fairly 'flat' and difficult to explain by FC. As noted above, there is the possibility that none of the mafic rocks sampled represents the basaltic parent, thus Barker et al.'s AFC model cannot be strictly ruled out. Parental basalts and/or their cumulate

products could remain hidden at depth, which is supported by the existence of a positive gravity anomaly exceeding +35 mgal that has been documented for the Pikes Peak batholith (Qureshy, 1958; cf Hutchinson, 1960).

We prefer a crustal anatexis model, rather than extreme evolution of mafic magmas via (A)FC processes, for the potassic granites. The tremendous volume of potassic granitoids in the batholith and the apparent lack of mafic rocks found in association with the potassic granites support crustal anatexis rather than AFC processes. Moderate degrees (~20–30%) of FC likely affected some potassic crustal melts [cf Fig. 7 (b)], as suggested by depletions in Ba, Sr and Eu in Figs. 5(e) and 7(b). Fractionation of minor amounts (~1%) of accessory minerals [e.g. zircon, monazite, titanite; cf Condie (1978)] is also suggested by unusual shapes of REE profiles in some of the Windy Point-type granites [Fig. 5 (f)]. However, we consider FC to be a secondary, rather than the dominant, petrogenetic process that affected the potassic granites.

8.2.4. Magma mixing/mingling models

There are no crustal sources evident that upon partial melting could have yielded melts with compositions comparable to the gray monzogranites (cf Figs. 10 and 11) and, as discussed above, none of the sampled Pikes Peak rocks appears to represent a parental magma that could have evolved by FC into the monzogranites. An alternative hypothesis is that the gray monzogranites represent products of magma mixing.

The monzogranites lie along fairly linear trends projected between Pikes Peak potassic granites and gabbros on Harker diagrams (e.g. Fig. 10). Binary mixing models involving Pikes Peak gabbros and potassic granites produce moderately good matches between calculated and observed monzogranite compositions for many elements, but Ba and Sr contents argue against models involving these end members [Fig. 7 (b)]. Furthermore, estimates of the proportion of the granitic end member range from ~75 to 90% in these models. At these proportions, mafic magma would likely be dispersed as enclaves within the silicic magma, rather than thoroughly mixed with it to produce a homogeneous hybrid (Sakuyama and Koyaguchi, 1984; Kouchi and Sunagawa, 1985;Sparks and Marshall, 1986). Mafic enclaves and other features indicating incomplete mixing have not been documented in the gray monzogranites. Alternatively, if the felsic end member was relatively hot [which is thought to be the case for many A-type granitic magmas; e.g. Turner et al. (1992)], then the likelihood of homogenization would have increased (Sparks and Marshall, 1986).

The problem of homogenization could be reduced if mixing occurred between intermediate and granitic end members, thus requiring smaller proportions of the latter. In particular, the melt composition generated from a ferrodiorite source [Figs. 7(b), 10 and 11] appears to be a plausible mixing end member. This mixing model is appealing, but we caution that the limited information regarding ferrodiorite melt products makes it rather speculative.

8.3. Tectonic setting

Details of the tectonic setting of the Pikes Peak batholith have not been well explained, but like most A-type, anorogenic granites (cf Turner et al., 1992), the batholith was probably emplaced in a region undergoing crustal extension. Adams and Keller (1994) noted that the period of formation of the ~1.2–1.0 Ga Mid-continent Rift (MCR) was also a time of widespread igneous activity in Texas and New Mexico, which they proposed was related to the MCR. Other evidence for extension in the southwestern US at 1.1 Ga includes diabase dikes in the Mojave region (Hammond, 1986). Adams and Keller (1994) compared the spatial distribution of ~1.1 Ga igneous activity to Mesozoic/Cenozoic rift features in Africa, including rift jumps, splays and offsets, and pointed out that the scale and complexity of the African rift system is comparable to the MCR. The ~1.07–1.09 Pikes Peak batholith is within distances comparable to those between the main axis of the African rift and off-axis jumps, splays and offsets [cf Fig. 8 in Adams and Keller (1994)]. As previously noted, six of the sodic plutons lie along NW–SE linears (Wobus, 1976) and intrusive centers within the PPG appear to have been fed by magmatic systems oriented in a NW–SE direction (Hutchinson, 1976). It appears that the Pikes Peak magmatic plumbing system was controlled by preexisting NW–SE fractures, which could have resulted from extension that affected the region at ~1.07–1.09 Ga. Unfortunately, our poor knowledge of the continent-scale plate tectonic geometry of North America during this time period precludes strong conclusions regarding the tectonic setting of the Pikes Peak batholith.

9. Summary and conclusions

The Pikes Peak batholith exhibits petrologic and geochemical characteristics typical of A-type, anorogenic granites. Major element compositions of Pikes Peak rocks are characterized by high Fe/(Fe+Mg) ratios and K_2O contents and low abundances of MgO and CaO. Trace elements exhibit large enrichments in incompatible elements and depletions in compatible elements, within the ranges typical of A-type granites. The ferromagnesian mineralogy of Pikes Peak syenites and granites includes anhydrous,

iron- and/or sodium-rich phases, which reflect crystallization under water- and oxygen-poor conditions. Compositions of magmas emplaced in late-stage intrusions include gabbro and diabase as well as granite, but unlike many A-type granites that occur in bimodal association with mafic rocks, the compositional range includes intermediate compositions.

Rocks of the late-stage intrusions can be differentiated into two series, sodic and potassic, on the basis of rock associations, ferromagnesian mineralogy and/or selected major and trace element characteristics of rocks with up to ~70–72 wt% silica. Nd isotopic ratios exhibit slight differences between the two series. The petrologic and geochemical differences exhibited by these two groups imply different petrogenetic histories. We believe that fractionation of mantle-derived magmas was the dominant process involved in the origin of the sodic series, whereas the origin of the potassic series was dominated by crustal anatexis.

The sodic series accounts for a very small proportion (<3%) of the exposed batholith but is characterized by a wide range of compositions, from gabbro to syenite to fayalite and sodic amphibole granite. Although we cannot rule out the possibility that Pikes Peak mafic magmas assimilated crust during ascent and/or emplacement, we suggest that the geochemical characteristics of the mafic rocks are the result of derivation from SSZ mantle sources. It appears that isotopic heterogeneity characterized the mantle source region, but it is difficult to address this heterogeneity in detail given the possibility of crustal assimilation.

The isotopic characteristics as currently documented for the regional Proterozoic crustal lithologies eliminate most of them as potential sources for the sodic granitoids by partial melting. In addition, we eliminate mafic lower crust, ferrodiorite, tonalite and residual crust as potential sources because melts generated from these materials do not have the high Fe/(Fe+Mg) ratios and/or alkali contents that characterize the sodic syenites and granites. The strong depletions in Ba and Sr observed in many sodic granitoids are also difficult to explain by melting of basalt, ferrodiorite or tonalite source rocks. The spectrum of compositions of the sodic series is proposed to be the result of fractionation of mantle-derived basaltic magmas. Other evidence in support of FC includes enrichments in incompatible elements and large depletions in compatible elements, relatively small volumes of sodic series granitoid magmas emplaced in the batholith, and low oxygen fugacities and high temperatures estimated for some sodic granitoid magmas. HFSE and REE concentrations in some sodic granitoid magmas could have been modified by accessory mineral fractionation, release of fluorine-rich volatiles, and/or formation of pegmatitic fluids.

If mafic magmas parental to the syenites and granites were derived from heterogeneous mantle sources characterized by $\epsilon_{Nd}(T)$ lower than depleted mantle, it is very difficult to estimate crust versus mantle contributions to the sodic granitoids. Neodymium isotopic data are permissive of contamination by lower crust, but those data and estimates of low oxygen fugacities preclude significant interactions between wall rocks (Frost and Frost, 1997) and sodic granitoid magmas. Sodic granitoids with low $\epsilon_{Nd}(T)$ values could be interpreted as depleted mantle + crust mixtures, whereas there may be no (or a small) crustal component if parental basalts were derived from SSZ or 'enriched' sources.

The potassic series includes fine-grained granites of the late-stage intrusions (Windy Point-type granites). The rocks are fairly restricted in composition (i.e. they are not associated with mafic rocks) and exhibit Nd isotopic characteristics similar to estimates for Colorado crust at ~1.08 Ga. On the basis of their isotopic and major and trace element characteristics, we interpret the late-stage potassic granites to be partial melts of tonalitic/granodioritic crust. Crustal sources composed of residual lower crust, as well as underplated basalts and their differentiates, are ruled out because such sources cannot produce melts with the high alkali contents observed in the late-stage potassic granites. Crystal fractionation affected some of the potassic magmas, but is considered to be a secondary, rather than the dominant, petrogenetic process.

The majority of the batholith is composed of PPG, dominantly pink, coarse-grained, 'rapakivi' granites, which share geochemical characteristics with the Windy Point-type granites. Because of this similarity, these granites are also inferred to have a crustal anatectic origin involving granodiorite/tonalite sources. We caution that this interpretation is somewhat speculative due to our limited sampling of this huge body of material (cf Fig. 1). However, crustal anatexis seems to be a more plausible model than fractionation of mantle-derived mafic magmas, which would require an enormous amount of unexposed cumulate rocks. Although the potassic granitoids may have little or no mantle material component, mantle-derived magmas likely provided the heat required for crust anatexis.

The gray monzogranite unit in the northern portion of the batholith exhibits lower silica and higher Sr, Ba and Eu contents than the pink PPG, and appears to be a plausible parental magma to at least some of the pink PPG granites. Possible origins of the monzogranites include higher degrees of melting of granodiorite/tonalite sources than required for the potassic granites, mixing with mafic and/or intermediate magmas, and/or crystal fractionation of mantle-derived basaltic magmas, but none of these hypotheses can be conclusively supported or ruled out.

The two main petrogenetic models proposed here, fractionation (+ minor assimilation of lower crust) of

basaltic magmas for the sodic series and tonalite anatexis for the potassic series, imply the existence of mafic rocks at depth. Some would be cumulates left from fractionation of basalts that generated syenitic and granitic magmas of the sodic series. Others would be solidified products of mantle-derived magmas, which provided heat input for crustal anatexis that generated granitic magmas of the potassic series. Exposures of mafic rocks in the batholith are small, but the positive gravity anomaly documented for the batholith (Qureshy, 1958) supports the existence of significant amounts of mafic rock at depth. Assuming that basalt fractionation played a direct role in petrogenesis of the sodic magmas, and that the potassic magmas required a major input of basaltic magma as a heat source, emplacement of the batholith represents a period of growth during which a large amount of juvenile, mantle-derived material was added to the crust.

Acknowledgements

The authors gratefully acknowledge the William M. Keck Foundation for its generous support of the Keck Geology Consortium, which sponsored the faculty-student research project that generated much of the data presented here. They thank Emily Giambalvo and Marnie Sturm for their input and insights on this project. D.S. thanks Trinity University for faculty development funds. J.D. and D.S. thank Dr Jim Wright at Rice University for access to and assistance in his laboratory in which some of the Sm–Nd isotopic data presented here were obtained. Access to XRF and/or ICP analytical facilities at the University of Massachusetts, Amherst College, and Franklin and Marshall College is gratefully acknowledged. The authors are also very grateful to the following individuals for their interest in this project and for useful discussions on the origin of the Pikes Peak batholith: Lawford Anderson; Calvin Barnes; Lori Bettison-Varga; Shelby Boardman; Peter Crowley; the late Sam Kozak; Hanna Nekvasil; Robert Schuster; and Steve Weaver. D.U. wishes to thank F.A. Barker, and the late R.M. Hutchinson for field expertise and assistance with sample selection, and the late W.N. Sharp for samples and access to unpublished maps and geochemical data. Constructive reviews by Elizabeth Anthony, David R. Nelson, Brian Marshall and Wayne Premo are gratefully acknowledged.

References

Adams, D.C., Keller, G.R., 1994. Possible extension of the Mid-continent Rift in west Texas and eastern New Mexico. Canadian Journal of Earth Sciences 31, 709–720.

Anderson, J.L., 1983. Proterozoic anorogenic granite plutonism of North America. Geological Society of America Memoir 161, 133–154.

Anderson, J.L., Morrison, J., 1992. The role of anorogenic granites in the Proterozoic crustal development of North America. In: Condie, K.C. (Ed.), Proterozoic Crustal Evolution. Elsevier, Amsterdam, pp. 263–299.

Barker, F., 1991. Comment on ‘‘A-type granites revisited: assessment of a residual source model’’. Geology 19, 1151.

Barker, F., Wones, D.R., Sharp, W.N., Desborough, G.A., 1975. The Pikes Peak Batholith, Colorado Front Range, and a model for the origin of the gabbro–anorthosite–syenite–potassic granite suite. Precambrian Research 2, 97–160.

Barker, F., Hedge, C., Millard, H., O’Neil, J., 1976. Pikes Peak Batholith: Geochemistry of some minor elements and isotopes, and implications for magma genesis. In: Epis, R.C., Weimer, R.J. (Eds.), in: Studies in Colorado Field Geology vol. 8. Colorado School of Mines Profession Contributions, Colorado, USA, pp. 44–56.

Barnes, C.G., Shannon, W.M., Kargi, H., 1999. Diverse Middle Proterozoic basaltic magmatism in west Texas. Rocky Mountain Geology 34 (2) in press.

Beane, R.J, 1993. Field relations, petrology and geochemistry of the Sugarloaf complex, Pikes Peak Batholith, Colorado. B.A. Honors Thesis, Williams College, Williamstown, MA, USA (unpublished).

Beard, J.S., Lofgren, G.E., 1991. Dehydration melting and water-saturated melting of basaltic and andesitic green-stones and amphibolites at 1, 3, and 6.9 kb. Journal of Petrology 32, 365–401.

Bickford, M.E., 1988. The accretion of Proterozoic crust in Colorado: igneous, sedimentary, deformational and metamorphic history. In: Ernst, W.G. (Ed.), in: Metamorphism and Crustal Evolution of the Western United States Rubey vol. 7. Prentice Hall, Englewood Cliff, NJ, pp. 411–430.

Bickford, M.E., Van Schmus, W.R., Zietz, I., 1986. Proterozoic history of the midcontinent region of North America. Geology 14, 492–496.

Bickford, M.E., Cullers, R.L., Shuster, R.D., Premo, W.R., Van Schmus, W.R., 1989. U–Pb zircon

geochronology of Proterozoic and Cambrian plutons in the Wet Mountains and southern Front Range, Colorado Proterozoic Geology of the Southern Rocky Mountains, Grambling, J.A., Tewksbury, B.J. (Eds.), Geological Society of America Special Paper 235, 49–64.

Bryant, B., McGrew, L.W., Wobus, R.A., 1981. Geologic map of the Denver 1° by 2° Quadrangle, north-central Colorado. US Geological Survey Map I-1163. US Geological Survey, Denver, CO, USA.

Campbell, I.H., Griffiths, F.W., 1990. Implications of mantle plume structure for the evolution of flood basalts. Earth and Planetary Science Letters 99, 79–92.

Carroll, M.R., Wyllie, P.J., 1990. The system tonalite–H_2O at 15 kbar and the genesis of calc-alkaline magmas. American Mineralogist 75, 345–357.

Charoy, B., Raimbault, L., 1994. Zr-, Th-, and REE-rich biotite differentiates in the A-type granite pluton of Suzhou (eastern China): the key role of fluorine. Journal of Petrology 35, 916–962.

Chastain, L., Noblett, J., 1994. Magma mingling in the anorogenic Proterozoic West Creek pluton, Pikes Peak Batholith, Colorado. Geological Society of America Abstracts with Programs 26, 8.

Clemens, J.D., Holloway, J.R., White, A.J.R., 1986. Origin of an A-type granite: experimental constraints. American Mineralogist 71, 317–324.

Collins, W.J., Beams, S.D., White, A.J.R., Chappell, B.W., 1982. Nature and origin of A-type granites with particular reference to southeastern Australia. Contributions to Mineralogy and Petrology 80, 189–200.

Condie, K.C., 1978. Geochemistry of Proterozoic granitic plutons from New Mexico, U.S.A. Chemical Geology 21, 131–149.

Creaser, R., Price, R., Wormald, R., 1991. A-type granites revisited: assessment of residual-source model. Geology 19, 163–166.

Davidson, J.P., 1996. Deciphering mantle and crustal signatures in subduction zone magmatism

(overview) Subduction Top to Bottom, Bebout, G.E., Scholl, D.W., Kirby, S.H., Platt, J.P. (Eds.), American Geophysical Union, Geophysical Monograph 96, 251–262.

Davis, C., 1993. A petrological and geochemical study of the gabbros and associated rocks from the Pikes Peak Batholith, Southern Front Range, Colorado. B.A. Thesis, Washington and Lee University, Lexington, VA, USA (unpublished).

DePaolo, D.J., 1981a. Neodymium isotopes in the Colorado Front Range and crust-mantle evolution in the Proterozoic. Nature 291, 193–196.

DePaolo, D.J., 1981b. Trace element and isotopic effects of combined wallrock assimilation and fractional crystallization. Earth and Planetary Science Letters 53, 189–202.

Ebadi, A., Johannes, W., 1991. Beginning of melting and com- position of first melts in the system Qz–Ab–Or–H_2O– CO_2. Contributions to Mineralogy and Petrology 106, 286–295.

Foland, K.A., Allen, J.C., 1991. Magma sources for Mesozoic anorogenic granites of the White Mountain magma series, New England, USA. Contributions to Mineralogy and Petrology 109, 195–211.

Frost, C.D., Frost, R.B., 1997. Reduced rapakivi-type granites: the tholeiite connection. Geology 25, 647–650.

Frost, R.B., Lindsley, D.H., Andersen, D.J., 1988. Fe–Ti oxide–silicate equilibria: assemblages with fayalitic olivine. American Mineralogist 73, 727–740.

Gable, D.J., 1980. The Boulder Creek Batholith, Front Range, Colorado. US Geological Survey. Professional Paper 1101

Giambalvo, E., 1993. Amphibole chemistry in alkaline igneous rocks of the Pikes Peak Batholith, Colorado. B.A. Honors Thesis, Amherst College, Amherst, MA, USA (unpublished).

Goldman, S., 1993. Geochemistry and petrography of the Mount Rosa intrusive center dikes, Pikes Peak Batholith, Colorado. B.A. Honors Thesis, The Colorado College, Colorado Springs, CO, USA

(unpublished).

Gross, E.B., Heinrich, E.W., 1966. Petrology and mineralogy of the Mount Rosa area, El Paso and Teller counties, Colorado III. Lamprophyres and mineral deposits. American Mineralogist 51, 1433–1442.

Gustavson, B., 1993. Trace element geochemistry of the fine-grained granite member of the Pikes Peak Batholith, as a key to identifying the batholith's tectonic history and source rock compositions. B.A. Honors Thesis, Carleton College, Northfield, MN, USA (unpublished).

Halliday, A.N., Davidson, J.P., Hildreth, W., Holden, P., 1991. Modeling the petrogenesis of high Rb/Sr silicic magmas. Chemical Geology 92, 107–114.

Hammond, J.G., 1986. Geochemistry and petrogenesis of Proterozoic diabase in the southern Death Valley region of California. Contributions to Mineralogy and Petrology 93, 312–321.

Harris, C., 1983. The petrology of lavas and associated plutonic inclusions of Ascension Island. Journal of Petrology 24, 424–470.

Harrison, T.M., Watson, E.B., 1984. The behavior of apatite during crustal anatexis: equilibrium and kinetic considerations. Geochimica et Cosmochimica Acta 48, 1464–1477.

Hawkesworth, C.J., Vollmer, R., 1979. Crustal contamination versus enriched mantle: $^{143}Nd/^{144}Nd$ and $^{87}Sr/^{86}Sr$ evidence from the Italian volcanics. Contributions to Mineralogy and Petrology 69, 151–165.

Hawkesworth, C.J., Hergt, J.M., Ellam, R.M., McDermott, F., 1991. Element fluxes associated with subduction related magmatism. Philosophical Transactions of the Royal Society of London Series A 335, 393–405.

Helz, R.T., 1976. Phase relations of basalts in their melting ranges at PH2 =5 kb. Part II. Melt compositions. Journal of Petrology 17, 139–193.

Hergt, J.M., Peate, D.W., Hawkesworth, C.J., 1991. The petro-genesis of Mesozoic Gondwana low-Ti flood basalts. Earth and Planetary Science Letters 105, 134–148.

Hoffman, P.F., 1988. United plates of America, the birth of a craton: Early Proterozoic assembly and growth of Laurentia. Annual Reviews of Earth and Planetary Science 16, 543–603.

Holloway, J.R., Burnham, C.W., 1972. Melting relations of basalt with equilibrium water pressure less than total pressure. Journal of Petrology 13, 1–29.

Huppert, H.E., Sparks, R.S.J., 1985. Cooling and contamination of mafic and ultramafic magmas during ascent through continental crust. Earth and Planetary Science Letters 74, 371–386.

Hutchinson, R.M., 1960. Structure and petrology of north end of Pikes Peak batholith, Colorado. In: Weimer, R.J., Haun, J.D (Eds.), Guide to the Geology of Colorado. Rocky Mountain Association of Geologists, pp. 170–180.

Hutchinson, R.M., 1972. Pikes Peak batholith and Precambrian basement rocks of the central colorado Front Range; their 700 million-year history 24th International Geologic Congress, Section 1. Precambrian Geology, 201–212.

Hutchinson, R.M., 1976. Granite-tectonics of Pikes Peak batholith. In: Epis, R.C., Weimer, R.J (Eds.), Studies in Colorado Field Geology vol. 8. Colorado School of Mines Professional Contributions, Colorado, USA, pp. 32–43.

Jenner, G.A., Cawood, P.A., Rautenschlein, M., White, W.M., 1987. Composition of back-arc basin volcanics, Valu-Fa Ridge, Lau Basin: evidence for a slab-derived component in their mantle source. Journal of Volcanology and Geother- mal Research 32, 209–222.

Karlstrom, K.E., Bowring, S.A., 1987. Early Proterozoic assembly of tectonostratigraphic terranes in southwestern North America. Journal of Geology 96, 561–576.

Kay, G., 1993. The petrology and geochemistry of the Mount Rosa granite, Pikes Peak Batholith. B.A. Thesis, The Colorado College, Colorado Springs, CO, USA (unpublished).

Kerr, A., Fryer, B.J., 1993. Nd isotope evidence for crust-mantle interaction in the generation of A-type

granitoid suites in Labrador, Canada. Chemical Geology 104, 39–60.

Kouchi, A., Sunagawa, I., 1985. A model for mixing basaltic and dacite magmas as deduced from experimental data. Contributions to Mineralogy and Petrology 89, 17–23.

LeRoex, A.P., 1985. Geochemistry, mineralogy and magmatic evolution of the basaltic and trachytic lavas from Gough Island, South Atlantic. Journal of Petrology 26, 149–186.

Loiselle, M.C., Wones, D.R., 1979. Characteristics and origin of anorogenic granites. Geological Society of America Abstracts with Program 11, 468.

Macdonald, R., McGarvie, D.W., Pinkerton, H., Smith, R.L., Palacz, Z.A., 1990. Petrogenetic evolution of the Torfajökull volcanic complex, Island I. Relationship between the magma types. Journal of Petrology 31, 429–459.

McKenzie, D.P., 1985. The extraction of magma from the crust and mantle. Earth and Planetary Science Letters 74, 81–91.

Mitchell, J.N., Scoates, J.S., Frost, C.D., Kolker, A., 1996. The geochemical evolution of anorthosite residual magmas in the Laramie anorthosite complex, Wyoming. Journal of Petrology 37, 637–660.

Patiño Douce, A.E., 1997. Generation of metaluminous A-type granites by low-pressure melting of calc-alkaline granitoids. Geology 25, 743–746.

Pearce, J.A., 1983. Role of sub-continental lithosphere in magma genesis at active continental margins. In: Hawkesworth, C.J., Norry, J.M. (Eds.), Continental Basalts and Mantle Xenoliths. Shiva, Nantwich, pp. 230–249.

Premo, W.R., Fanning, C.M., 1997. U–Pb zircon ages for the big Creek gneiss, Wyoming and the Boulder Creek batholith, Colorado: implications for the timing of early Proterozoic accretion of the northern Colorado province. Geological Society of America Abstracts with Programs 29, A407.

Qureshy, M.N., 1958. Gravity anomalies and a suggested genesis for Pikes Peak batholith, Front Range Colorado (abs.). Geological Society of America Bulletin 69, 1740.

Reed Jr, J.C., Bickford, M.E., Premo, W.R., AleinikoV , J.N., Pallister, J.S., 1987. Evolution of the Early Proterozoic Colorado province: constraints from U–Pb geochronology. Geology 15, 861–865.

Reichen, L.E., Fahey, J.J., 1962. An improved method for the determination of FeO in rocks and minerals including garnet. US Geological Survey Bulletin 1144B, 1–5.

Roberts, M.P., Clemens, J.D., 1993. Origin of high-potassium, calc-alkaline, I-type granitoids. Geology 21, 825–828.

Rock, N.M.S., 1991. Lamprophyres. Van Nostrand Reinhold, New York.

Rollinson, H., 1993. Using Geochemical Data: Evaluation, Presentation, Interpretation. Longman Scientific and Technical, Essex.

Rudnick, R.L., Presper, T., 1990. Geochemistry of intermediate- to high-pressure granulites. In: Vielzeuf, D., Vidal, Ph. (Eds.), Granulites and Crustal Evolution. Kluwer Academic Publishers, Netherlands, pp. 523–550.

Rushmer, T., 1991. Partial melting of two amphibolites: contrasting experimental results under fluid-absent conditions. Contributions to Mineralogy and Petrology 107, 41–59.

Sage, R.P., 1966. Geology and mineralogy of the Cripple Creek syenite stock, Teller County, Colorado. Master's thesis, Colorado School of Mines, Golden, CO (unpublished).

Sakuyama, M., Koyaguchi, T., 1984. Magma mixing in mantle xenolith-bearing calc-alkalic ejecta, Ichinomegata volcano, northeastern Japan. Journal of Volcanology and Geothermal Research 22, 199–224.

Saltoun, B., 1993. A petrologic and geochemical analysis of the fayalite-bearing granitoids, Mount Rosa intrusive center, Colorado. B.A. Thesis, The College of Wooster, Wooster, OH, USA (unpublished).

Saunders, A.D., Tarney, J., 1984. Geochemical characteristics of basaltic volcanism within back-arc

basins. In: Kokelaar, B.P., Howells, M.F. (Eds.), Marginal Basin Geology, Geo- logical Society of London, Special Publication 16, 59–76.

Schärer, U., Allègre, C.J., 1982. Uranium–lead system in fragments of a single zircon grain. Nature 295, 585–587.

Scoates, J.S., Frost, C.D., Mitchell, J.N., Lindsley, D.H., Frost, R.B., 1996. Residual-liquid origin for a monzonitic intrusion in a mid-Proterozoic anorthosite complex: the Sybille intrusion, Laramie anorthosite complex, Wyoming. Geological Society of America Bulletin 108, 1357–1371.

Scott, G., Taylor, R., Epis, R., Wobus, R., 1978. Geologic Map of the Pueblo 1°×2° Quadrangle, South-central Colorado. in: US Geological Survey Miscellaneous Investigations Series Map I-1022. US Geological Survey, Denver, CO, USA.

Simmons, W.B., Lee, M.T., Brewster, R.H., 1987. Geochemistry and evolution of the South Platte granite–pegmatite system, Jefferson County, Colorado. Geochimica et Cosmochimica Acta 51, 455–471.

Skjerlie, K.P., Johnston, A.D., 1993. Fluid absent melting behavior of an F-rich tonalitic gneiss at mid-crustal pressures: implications for the generation of anorogenic granites. Journal of Petrology 34, 785–815.

Sparks, R.S.J., Marshall, L.A., 1986. Thermal and mechanical Webster, J.D., Holloway, J.R., 1990. Partitioning of F and Cl constraints on mixing between mafic and silicic magmas. Journal of Volcanology and Geothermal Research 29, 99–124.

Spulber, S.D., Rutherford, M.J., 1983. The origin of rhyolite and plagiogranite in oceanic crust: an experimental study. Journal of Petrology 24, 1–25.

Stewart, J., 1994. A mineralogical geochemical and petrogenetic study of the syeno- and monzo-granites of the Pikes Peak batholith in the southern Front Range of Colorado. Bachelor's thesis, Beloit College, Beloit, WI, USA (unpublished).

Sun, S.S., 1980. Lead isotopic study of young volcanic rocks from mid-ocean ridges, ocean islands and island arcs. Philosophical Transactions of the Royal Society of London, Series A 297, 409–445.

Sylvester, P.J., 1989. Post-collisional alkaline granites. Journal of Geology 97, 261–280.

Tatsumi, Y., Hamilton, D.L., Nesbitt, R.W., 1986. Chemical characteristics of fluid phase released from a subducted lithosphere and the origin of arc magmas: evidence from high-pressure experiments and natural rocks. Journal of Volcanology and Geothermal Research 29, 293–309.

Taylor, S.R., McClennan, S.M., 1985. The Continental Crust: its Composition and Evolution. Blackwell, Oxford.

Thompson, R.N., Dickin, A.P., Gibson, I.L., Morrison, M.A., 1982. Elemental fingerprints of isotopic contamination of Hebridean Palaeocene mantle-derived magmas by Archaean sial. Contributions to Mineralogy and Petrology 79, 159–168.

Turner, S.P., Foden, J.D., Morrison, R.S., 1992. Derivation of some A-type magmas by fractionation of basaltic magma: an example from the Padthaway Ridge, South Australia. Lithos 28, 151–179.

Watson, E.B., Harrison, T.M., 1983. Zircon saturation revisited: temperature and composition effects in a variety of crustal magma types. Earth and Planetary Science Letters 64, 295–304.

Weaver, B.L., 1991. The origin of ocean island basalt end- member compositions: trace element and isotopic constraints. Earth and Planetary Science Letters 104, 381–397.

Weaver, B., Tarney, J., 1984. Empirical approach to estimating the composition of the continental crust. Nature 310, 575–577.

Webster, J.D., Holloway, J.R., 1990. Partitioning of F and Cl between magmatic hydrothermal fluids and highly evolved granitic magmas. In: Hannah, J.L., Stein, H.J. (Eds.), Ore-bearing granite systems, petrogenesis and mineralizing processes, Geological Society of America Special Paper 246, 21–34.

Whalen, J.B., Currie, K.L., Chappell, B.W., 1987. A-type granites: geochemical characteristics, discrimination and petro- genesis. Contributions to Mineralogy and Petrology 95,407–419.

Wickham, S.M., 1987. The segregation and emplacement of granitic magmas. Journal of the Geological

Society 144,281–297.

Wilson, M., 1989. Igneous petrogenesis. Unwin Hyman, London.

Wobus, R.A., 1976. New data on potassic and sodic plutons of the Pikes Peak batholith, central Colorado. In: Epis, R.C., Weimer, R.J. (Eds.), Studies in Colorado Field Geology vol. 8. Colorado School of Mines Professional Contributions, Colorado, USA, pp. 57–67.

Wobus, R.A., Anderson, R.S., 1978. Petrology of the Precambrian intrusive center at Lake George, southern Front Range, Colorado. Journal of Research of the US Geological Survey 6, 81–94.

Wyllie, P.J., 1984. Constraints imposed by experimental petrology on possible and impossible magma sources and products. Philosophical Transactions of the Royal Society of London, Series A 310, 439–456.

Figure 1:

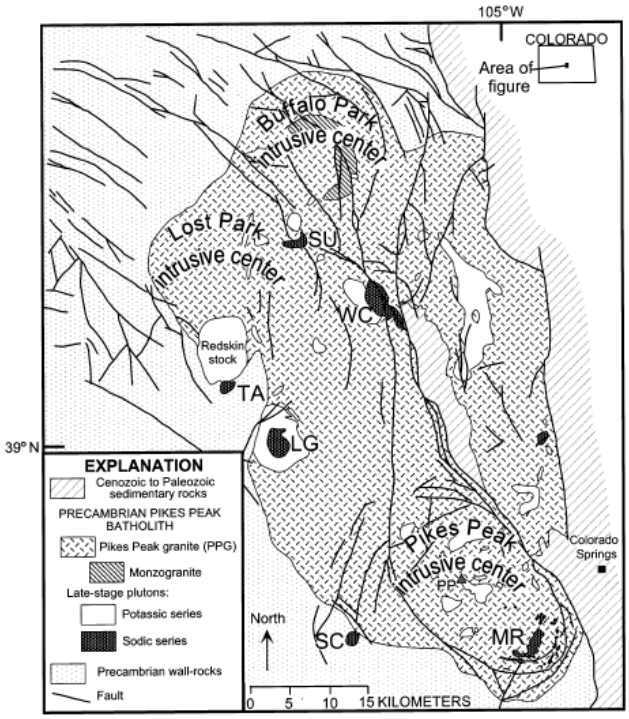

Fig. 1. Geologic map of the Pikes Peak batholith [after Bryant et al. (1981); and Scott et al. (1978)]. Late-stage alkalic intrusions include Sugarloaf (SU), Tarryall (TA), West Creek (WC), Lake George (LG), Spring Creek [SC; sometimes called the Cripple Creek stock, e.g. Sage (1966)], and the Mount Rosa intrusive complex (MR). The main phase of the batholith is generally composed of coarse-grained pink granite (associated with minor gray monzogranite) referred to here as PPG. PP, the summit of Pikes Peak.

Table 1:

Table 1
Major rock types of the Pikes Peak batholith and samples of this study (cf Fig. 1 and Tables 2–11)

Rock types[a]	Samples of this study[b]
PPG	
Pink PPG:	
Dominantly pink, medium to coarse, biotite ± amphibole syenogranite with large potassium feldspar grains	GM-7-BG; WP-33-BG; 85BP4; SPD1R[c]
Gray monzogranite:	
Gray, medium to coarse, biotite ± amphibole monzogranite; some contain plagioclase megacrysts	GM-8-JS; GM-19-JS; D-22-JS; GM-30-JS; WB-42-JS; GM-6-JS; P-26-JS; P-2-JS; GM-23-JS
Late-stage plutons:	
Potassic series:	
K/Na = 0.95 – 2.05	
Fine to medium, (commonly) porphyritic biotite granite and minor quartz monzonite	
Found in small, unnamed stocks scattered throughout the batholith	P-2-BG; GM-5-BG; GM-8-BG; WC-9-BG; WC-10-BG; GM-17-BG; LG-21-BG; C-24-BG; DM-26-BG; HM-27-BG; HM-28-BG; PP-31-BG; PP-31-JD; PP-34-BG; MBC-37-BG; MBC-38-BG; MBC-39-BG; GM-40-BG; CL-41-BG; GM-12-BG; GM-13-BG; PP-32-BG
Other potassic granitoids found at Tarryall, Lake George and the Redskin stock	86TQM; 86LG7; 85RS2
Sodic series:	
K/Na = 0.32 – 1.36	
Found in ring dikes and stocks of seven of the late-stage intrusions (cf Fig. 10)	
Rock types include:	
(Rare) anorthosite	(not included in this study)
Gabbro	T-34-CD; T-30-CD; 86TARG; LG-12-JD; LG-22-CD; LG-23-CD; 86LG6; CCN-19-CD; CCN-19B-CD
Mafic (diabase) dikes	MBC-8-SG; S71PPG29; MBC-9-SG; MBC-51-SG; MBC-20-SG; MBC-74-SG; MBC-10-SG; MBC-11-SG; MBC-83-SG; MBC-85-SG
Granodiorite and quartz monzonite	(not included in this study)
Intermediate dikes	MBC-77-SG; MBC-79-SG; MBC-56-SG; S71PPG2A; S71PPG21
Syenites and quartz syenites	LG-10-JD; 86LG5; WC-5-JD; GM-12-RB; GM-18-RB; GM-19-RB; GM-21-RB; GM-23-RB; GM-31-RB; GM-34-RB; GM-35-RB; GM-36-RB
Fayalite-bearing granite	MBC-20-BS; MBC-6-BS; MBC-7-BS; MBC-8-BS; MBC-19-BS; B65DSR; B65F; 86LG4
Sodic-amphibole and/or biotite granite	MBC-9-GK; MBC-12-GK; MBC-6-GK; MBC-10-GK; MBC-15-GK; 85MRI; 85TG1; 85AM1

[a] For additional details of the occurrence, age relations and petrography of rocks of the Pikes peak batholith, see Hutchinson (1960, 1972, 1976), Barker et al. (1975, 1976), Wobus (1976), Wobus and Anderson (1978), Beane (1993), Davis (1993), Goldman (1993), Gustavson (1993), Kay (1993), Saltoun (1993), Stewart (1994) and Chastain and Noblett (1994).

[b] Sample location information is available from the senior author.

[c] The very limited sampling here of the voluminous pink PPG is mainly for comparative purposes.

Table 2:

Table 2
Major and trace element analyses of gabbros of the sodic series, Pikes Peak batholith

Sample No.	T-34-CD	T-30-CD	86TARG	LG-12-JD	LG-22-CD	LG-23-CD	86LG6	CCN-19-CD	CCN-19B-CD
Intrusion	Tarryall	Tarryall	Tarryall	Lake George	Lake George	Lake George	Lake George	Spring Creek	Spring Creek
SiO_2	50.98	50.93	46.50	47.2	47.57	47.68	47.70	45.80	44.27
TiO_2	2.61	2.81	4.98	2.95	2.99	2.95	3.05	1.41	4.76
Al_2O_3	16.24	15.32	16.31	14.9	14.35	14.50	14.80	14.50	13.35
Fe_2O_3	1.95	3.14	1.59	12.8	1.84	2.31	1.99	12.60	3.35
FeO	8.30	9.76	10.64		10.52	9.79	10.80		13.76
MnO	0.20	0.22	0.25	0.25	0.24	0.24	0.27	0.20	0.24
MgO	2.59	2.77	3.82	4.15	4.26	4.40	4.50	11.50	4.50
CaO	8.15	7.67	8.37	6.63	7.06	6.86	6.68	8.56	7.64
Na_2O	4.07	3.75	3.82	4.04	4.38	4.42	4.33	1.26	3.65
K_2O	1.98	2.08	1.38	2.44	2.61	2.63	2.54	1.08	1.56
P_2O_5	1.77	1.50	2.01	2.43	2.78	2.53	2.40	0.51	1.67
Sum	98.84	99.94	99.67	97.79	98.60	98.31	99.06	97.42	98.75
Mg No.	31.5	28.2	36.0	39.1	38.4	39.8	38.9	64.4	32.3
Ni	60	2			4	6		280	5
Cr	5.1	18		5.9	15.0	8.0		650	9
V		121			115	114			158
Sc	24.9	27		14.8	21.0	20.0		31.1	22.9
Co	21	27		10	28	28		65	47
Zn	140			140				190	160
Ga				29				28	28
Cs	1.7			1.4				14.6	1.2
Ba	1500	1225		1500	1415	1394	1500	1200	880
Rb	60	54		49	47	49	57	62	23
Th	4			14			8	3	3
Sr	800	666		634	688	671	640	630	580
Zr		212		230	236	240		180	191
Nb				46			17	10	21
Hf	5.3			13.0				5.3	5.6
Ta	1.4			2.0				0.5	1.2
La	52.3	50		88.7	67.0	66.0	67	36.3	35.5
Ce	115	107		179	133	130	120	76	80
Nd	60			86			75	37	45
Sm	14.4			16.7			14.9	7.7	10.6
Eu	4.42			3.47				2.07	3.36
Tb	2.0			2.1				1.0	1.6
Yb	4.48	5.1		7.14	5.10	5.00	6	2.10	3.75
Lu	0.63			1.09				0.30	0.54
Y		62		43	59	60	52	12	55
U				3.0				0.9	0.5
Be		1.1			1.1	1.0			

Table 3:

Table 3
Major and trace element analyses of mafic dikes of the sodic series, Pikes Peak batholith

Sample No.	MBC-8-SG	S71PPG29	MBC-9-SG	MBC-51-SG	MBC-20-SG	MBC-74-SG	MBC-10-SG	MBC-11-SG	MBC-83-SG	MBC-85-SG
Intrusion	Mt. Rosa	Mt. Rosa	Mt. Rosa	Mt. Rosa	Mt. Rosa	Mt. Rosa	Mt. Rosa	Mt. Rosa	Mt. Rosa	Mt. Rosa
SiO_2	45.81	44.30	45.58	45.08	46.69	50.90	52.79	52.33	47.02	52.44
TiO_2	3.50	3.42	3.45	3.33	3.44	2.49	2.21	2.17	3.49	2.44
Al_2O_3	16.18	15.40	16.04	13.74	16.63	14.38	15.10	14.97	16.22	14.92
Fe_2O_3	16.34	3.97	16.88	16.99	16.50	14.97	13.20	13.12	16.03	13.97
FeO		11.00								
MnO	0.24	0.23	0.30	0.26	0.23	0.39	0.40	0.39	0.27	0.56
MgO	5.35	5.57	5.27	6.37	4.79	2.37	2.20	2.22	4.62	2.29
CaO	7.42	6.91	6.80	5.74	6.45	5.13	4.06	4.00	7.07	5.03
Na_2O	3.68	3.49	2.71	2.95	3.41	4.24	4.32	4.60	3.38	4.39
K_2O	2.23	2.43	2.67	3.59	2.70	3.16	3.86	3.47	2.07	3.27
P_2O_5	0.63	0.83	0.62	0.62	0.65	1.32	1.01	1.04	0.60	1.26
Sum	101.38	97.55	100.32	98.67	101.49	99.35	99.15	98.31	100.77	100.57
Mg No.	39.3	40.5	38.2	42.6	36.5	23.9	24.8	25.1	36.3	24.5
Ni	98		81	57	14			33	7	17
Cr	25		129	86	3	41		79	23	18
V	70		85	83	73				89	
Sc	18.5					18.9				
Co	47		48	50	39	44	4	8	36	6
Zn	340		852	360	381	260	271	247	217	421
Ga	30									
Cs	9.3					8.6				
Ba	910	770				740				
Rb	187	218	225	496	250	130	103	85	118	147
Th	1	4				2				
Sr	527	560	423	343	491	349	330	358	453	363
Zr	240		237	247	269	302	436	445	277	335
Nb	20	11	26	36	27	50	85	83	30	56
Hf	6.3					7.9				
Ta	1.2					1.4				
La	29.7	35				30.2				
Ce	66	58				68				
Nd	37	43.2				36				
Sm	8.6	9.8				8.5				
Eu	2.77					3.32				
Tb	1.2					1.1				
Yb	2.85	5				3.75				
Lu	0.40					0.52				
Y	31	36	65	126	74	73	87	81	43	84
U	0.9									

Table 4:

Table 4
Major and trace element analyses of intermediate dikes of the sodic series, Pikes Peak batholith

Sample No.	MBC-77-SG	MBC-79-SG	MBC-56-SG	S71PPG2A	S71PPG21
Intrusion	Mount Rosa	Mount Rosa	Mount Rosa	Mount Rosa	Mount Rosa
SiO_2	60.86	59.94	65.04	59.0	58.6
TiO_2	1.11	1.19	0.59	1.12	1.17
Al_2O_3	15.48	15.48	13.93	13.6	14.7
Fe_2O_3	9.40	9.67	6.91	2.38	2.16
FeO				8.46	7.23
MnO	0.31	0.34	0.25	0.44	0.35
MgO	0.70	0.56	0.00	0.48	0.83
CaO	2.86	2.89	1.49	3.07	3.09
Na_2O	4.80	5.07	5.27	4.83	4.78
K_2O	4.82	4.69	4.86	4.93	4.79
P_2O_5	0.25	0.27	0.01	0.24	0.39
Sum	100.59	100.10	98.35	98.55	98.09
Mg No.	12.9	10.3	0.0	7.5	13.9
Ni					
Cr	7.6				
V					
Sc	33.6				
Co	3.3	1.0			
Zn	250	286	373		
Ga					
Cs	1.2				
Ba	2500			450	2300
Rb	220	161	251	162	121
Th	11			21	8
Sr	97	105	2	40	110
Zr	747	746	1458		
Nb	104	87	203	160	77
Hf	19.0				
Ta	4.0				
La	112			200	100
Ce	220			390	200
Nd	105			208.3	112.6
Sm	19.5			40.1	22.9
Eu	5.23				
Tb	2.7				
Yb	9.82			20	10
Lu	1.45				
Y	124	103	211	160	91

Table 5:

Table 5
Major and trace element analyses of syenites and quartz syenites of the sodic series, Pikes Peak batholith; ND, not detected

Sample No.	LG-10-JD	86LG5	WC-5-JD	GM-12-RB	GM-18-RB	GM-19-RB	GM-21-RB	GM-23-RB	GM-31-RB	GM-34-RB	GM-35-RB	GM-36-RB
Intrusion	Lake George	Lake George	West Creek	Sugar-loaf	Sugar-loaf	Sugar-loaf	Sugar-loaf	Sugar-loaf	Sugar-loaf	Sugar-loaf	Sugar-loaf	Sugar-loaf
SiO_2	68.4	61.7	64.1	63.79	63.21	61.44	60.77	63.41	72.24	62.61	61.53	65.75
TiO_2	0.29	0.71	0.18	0.33	0.47	0.89	0.79	0.36	0.18	0.53	0.68	0.13
Al_2O_3	14.7	16.6	17.3	16.83	15.41	15.18	14.89	16.09	13.17	15.11	15.45	17.22
Fe_2O_3	2.93	1.07	3.74	5.12	6.79	6.64	8.11	6.15	3.19	7.41	7.19	2.83
FeO		4.46										
MnO	0.10	0.20	0.19	0.12	0.26	0.27	0.32	0.22	0.11	0.29	0.31	0.09
MgO	0.07	0.54	0.14	0.15	0.19	0.79	0.64	0.20	0.08	0.20	0.46	0.11
CaO	0.76	2.03	1.62	1.04	1.30	2.00	1.89	1.12	0.62	1.46	1.80	1.30
Na_2O	5.57	5.32	6.73	6.91	6.46	6.32	6.54	6.67	4.90	6.41	6.67	7.22
K_2O	4.86	5.76	5.03	5.08	5.44	5.29	4.94	5.62	4.81	5.35	5.17	5.35
P_2O_5	0.03	0.13	0.03	0.04	0.13	0.37	0.30	0.03	0.01	0.10	0.21	0.03
Sum	97.71	98.52	99.06	99.41	99.68	99.19	99.19	99.87	99.31	99.47	99.47	100.02
Mg No.	4.5	15.1	6.9	5.3	5.3	19.1	13.4	6.0	4.5	5.1	11.3	6.9
Ni				7	6	12	7	5	4	7	10	7
Cr	2.1		5.1	1.0	2.0	ND	ND	ND	1	ND	ND	1
V				ND	1	3	4	ND	ND	2	1	ND
Sc	3.6		3.9	3.5	8.8	14.8					10.9	
Co	1.7		1.7	1.9	1.7	3.1					2.1	
Zn	110		90	126	204	145	215	177	165	230	210	112
Ga	41		37	37	35	28	31	35	31	35	33	38
Cs	0.6		0.6	0.5	1.3	0.9					0.7	
Ba	200	1400	220	48	140	1176	813	94	168	136	592	253
Rb	166	88	137	125	218	262	189	181	168	221	176	175
Th	33	5	24	12	11	8	6	4	5	8	15	9
Sr	14	130	25	8	16	86	62	16	10	16	53	28
Zr	430		1600	364	218	193	127	114	78	200	204	191
Nb	90	50	73	259	131	154	146	98	59	136	170	83
Hf	14		33.0	7.0	7.1	6.1					4.9	
Ta	7.2		3.9	13.0	5.3	11.0					8.7	
La	226.0	59	231.0	104.0	109.0	96.0					332	
Ce	402	110	402	198	205	181	178	438	90	91	570	81
Nd	146	58.5	138	73	85	84					200	
Sm	22.2	10.6	21.1	12.0	14.5	16.3					29.1	
Eu	1.49		0.71	0.66	1.25	2.80					2.72	
Tb	2.6		2.1	1.5	1.6	2.3					2.8	
Yb	9.65	4	8.61	5.06	6.71	6.41					7.00	
Lu	1.46		1.41	0.80	1.13	0.90					1.00	
Y	93	36	64	53.9	38.5	72.3	47.2	21.4	19.6	36.1	69.4	56
U	3.7		3.4	4.6	2.1	1.0	1.0	0.5	0.0	1.0	1.5	2.5

Table 6:

Table 6
Major and trace element analyses of fayalite-bearing granites of the sodic series, Pikes Peak batholith; ND, not detected

Sample No.	MBC-20-BS	MBC-6-BS	MBC-7-BS	MBC-8-BS	MBC-19-BS	B65DSR	B65F	86LG4
Intrusion	Mount Rosa	Mount Rosa	Mount Rosa	Mount Rosa	Mount Rosa	Mount Rosa	Mount Rosa	Lake George
SiO_2	68.9	68.9	70.2	70.50	71.25	69.9	69.09	70.1
TiO_2	0.37	0.28	0.34	0.26	0.30	0.27	0.37	0.18
Al_2O_3	14.3	13.9	13.3	13.03	14.43	13.6	14	14.3
Fe_2O_3	3.86	3.25	3.73	0.97	0.72	0.76	0.7	1.87
FeO				2.24	2.50	2.84	3.33	1.17
MnO	0.12	0.11	0.13	0.11	0.10	0.09	0.14	0.1
MgO	0.15	0.11	0.12	ND	ND	0.11	0.1	0.03
CaO	1.43	1.23	1.09	1.09	1.06	1.12	1.35	0.54
Na_2O	4.62	4.50	4.80	4.20	3.83	4.14	4.36	5.08
K_2O	5.15	4.88	4.85	5.32	5.43	5.39	5.43	5.38
P_2O_5	0.06	0.04	0.04	0.01	0.00	0.02	0.04	0.02
Sum	98.96	97.20	98.60	97.72	99.62	98.24	98.91	98.77
Mg No.	7.1	6.3	6.0	0.0	0.0	5.3	4.3	1.8
Ni	3	4	2	2	2			
Cr	5	5	4		3			
V	2	1	1	2	1			
Sc	8.6	4.7	4.0	6.0	6.4			
Co	2.1	1.8	1.7	0.6	0.7			
Zn	150	110	160	92	96			
Ga	35	35	40	30	28			
Cs	2.4	3.5	3.6					
Ba	681	508	186	664	617	560		180
Rb	239	317	287	275	256	278		202
Th	28	32	41			47		29
Sr	31	28	1	27	22	41		12
Zr	845	407	823	549	626			
Nb	84	79	100	75	76	31		13
Hf	21	15	22					
Ta	4.3	5.6	7.3					
La	80.8	110	142	136	173	160		170
Ce	168	213	276	246	305	300		280
Nd	83	89	117			123.6		108
Sm	17.9	16.8	22.3			22		16.7
Eu	1.99	1.74	1.23					
Tb	2.8	2.6	3.6					
Yb	12.7	12.0	16.8	14.9	16.8	14		8
Lu	1.99	1.86	2.57					
Y	171	113	173	115	160	110		62
U	6.2	7.9	11.6					
Be	6.0	7.7	12.6	5.7	9.9			

Table 7:

Table 7
Major and trace element analyses of sodic amphibole- and/or biotite-bearing granites of the sodic series, Pikes Peak batholith; ND, not detected

Sample No.	MBC-9-GK	MBC-12-GK	MBC-6-GK	MBC-10-GK	MBC-15-GK	85MRI	85TG1	85AM1
Intrusion	Mount Rosa	Mount Rosa	Mount Rosa	Mount Rosa	Mount Rosa	Mount Rosa	Mount Rosa	Mount Rosa
SiO_2	74.7	74.6	74.79	73.25	77.78	71.3	73.1	72.8
TiO_2	0.18	0.10	0.14	0.43	0.09	0.28	0.23	0.23
Al_2O_3	11.2	11.2	12.29	14.22	11.50	12.1	11.9	12.2
Fe_2O_3	4.56	4.33	2.80	4.38	2.21	1.04	1.07	1.25
FeO						2.97	2.25	1.84
MnO	0.08	0.09	0.04	0.09	0.02	0.1	0.07	0.05
MgO	0.09	0.05	0.11	0.10	ND	0.05	0.02	0.11
CaO	0.13	0.22	0.89	0.18	0.17	0.91	0.71	0.74
Na_2O	4.55	4.39	4.16	4.00	3.64	4.18	3.36	3.71
K_2O	4.08	4.72	3.88	5.19	4.59	4.96	5.1	5.2
P_2O_5	0.02	0.02	ND	ND	ND	0.02	ND	ND
Sum	99.59	99.72	99.09	101.84	100.00	97.91	97.81	98.13
Mg No.	3.8	2.2	7.2	4.1	0.0	2.2	1.1	6.2
Ni			9					
Cr	6.2							
V	12	5	8	23	4			
Sc	3.0	3.8						
Co	1.1	1.4	8.0	4.0	6.0			
Zn	304	320	440	221	149			
Ga	41	39	43	39	37			
Cs	0.8	0.6						
Ba	80	80	61	119	84	86	93	190
Rb	285	238	471	227	282	340	270	334
Th	2.2	5.7				58	39	61
Sr	6	7	29	4	6	22	15	17
Zr	103	230	1680	265	359			
Nb	18	40	290	35	23	12	17	13
Hf	3.6	7.6						
Ta		3.9						
La	149	79.3				220	210	190
Ce	266	158				400	370	340
Nd	108	66				159	169	143.5
Sm	16.9	12.5				29	30	25.8
Eu	0.40	0.44						
Tb	1.9	1.9						
Yb	3.96	5.53				17	15	16
Lu	0.74	0.94						
Y	92	78	352	14	42	160	140	130
U	0.4	1.5						

Table 8:

Table 8
Major and trace element analyses of Windy Point-type granites of the potassic series, Pikes Peak batholith

Sample No.	P-2-BG	GM-5-BG	GM-8-BG	WC-9-BG	WC-10-BG	GM-17-BG	LG-21-BG	C-24-BG	DM-26-BG	HM-27-BG	HM-28-BG	PP-31-BG	PP-31-JD	PP-34-BG	MBC-37-BG	MBC-38-BG	MBC-39-BG	GM-40-BG	CL-41-BG	GM-12-BG	GM-13-BG	PP-32-BG
SiO_2	72.91	70.65	73.13	71.57	74.26	74.20	72.67	77.50	73.27	74.11	75.50	73.51	72.50	73.59	70.05	72.18	75.00	73.14	75.59	69.48	75.60	76.03
TiO_2	0.34	0.44	0.34	0.16	0.22	0.16	0.13	0.15	0.28	0.22	0.12	0.25	0.27	0.16	0.34	0.27	0.12	0.26	0.21	0.74	0.21	0.04
Al_2O_3	12.86	13.85	12.58	14.00	12.64	12.35	13.05	11.34	12.55	12.57	13.01	13.05	13.70	12.95	14.66	13.85	12.41	13.04	11.92	13.18	12.49	12.53
Fe_2O_3	3.39	3.95	2.83	2.46	2.53	2.32	2.55	1.91	2.75	1.81	1.41	2.42	2.32	1.96	2.75	1.82	1.41	2.42	2.29	4.59	1.94	1.02
FeO																						
MnO	0.06	0.10	0.04	0.02	0.05	0.02	0.04	0.02	0.04	0.04	0.02	0.03	0.04	0.06	0.04	0.03	0.03	0.04	0.06	0.10	0.04	0.03
MgO	0.23	0.45	0.25	0.19	0.12	0.09	0.09	0.12	0.19	0.13	0.11	0.23	0.29	0.12	0.66	0.50	0.08	0.20	0.16	0.67	0.15	0.05
CaO	0.76	1.16	0.98	0.84	0.95	0.56	0.80	0.58	0.70	0.85	0.71	1.03	1.23	0.89	1.49	0.57	0.80	0.82	0.61	1.85	0.67	0.36
Na_2O	3.03	3.96	3.04	4.64	3.33	3.06	4.38	2.49	2.91	3.23	3.44	3.37	3.58	3.54	3.78	2.93	3.40	3.20	2.65	3.17	3.15	3.96
K_2O	5.75	5.08	5.58	4.95	5.17	5.51	4.74	5.71	5.85	5.69	5.24	5.32	5.09	5.24	5.00	6.29	5.42	5.53	5.51	5.09	5.40	4.56
P_2O_5	0.06	0.12	0.04	0.01	0.03	0.01	0.01	0.01	0.04	0.01	0.01	0.06	0.06	0.01	0.13	0.13	0.01	0.03	0.02	0.28	0.03	0.01
Sum	99.39	99.76	98.81	98.84	99.30	98.28	98.46	99.83	98.58	98.66	99.57	99.27	99.08	98.52	98.90	98.57	98.68	98.68	99.02	99.15	99.68	98.59
Mg No.	11.8	18.4	14.9	13.3	8.6	7.1	6.5	11.1	12.0	12.5	13.4	15.8	19.8	10.8	32.2	35.2	10.1	14.1	12.2	22.4	13.3	8.8
Ni		4	6	2	4	5	1	4	2	5	3	8		3	6	2	8	6	3			
Cr		0.8	4.0	1.6		2.2		0.3		0.6	1.0	4.3		0.1	12.0	3.8	2.4	1.9	0.9			
V	6.3	4.7	12.0	2.5	2.4	1.3	1.8	2.2	4.0	3.7	3.2	5.6		3.0	29.0	13.7	0.7	4.8	2.9			
Sc	6.9	8.7	4.1	3.0	4.2	4.0	3.7	2.0	4.1	4.7	2.0	4.2	2.3	2.9	3.6	5.5	3.8	5.7	3.5			
Co	3.0	3.4			1.1	1.0	1.4		1.7	1.1	1.5	2.0	1.3		5.2		1.0					
Zn	90	120	50	40	90	60	60	49	50	50	60	40		46	90		40	58	52			
Ga		26	23	28	26	26		22			22		32	25	27			26	21			
Cs	1.1	2.7			2.5	2.0	4.2		1.2	2.9	6.6	3.0	1.8		2.5		3.6					
Ba	635	918	444	78	550	298	215	200	297	394	616	568	690	390	1061	574	252	526	604			
Rb	170	250			270	290	320		190	260	290	310	294		250		410					
Th	37	32			35	56	61		42	40	52	50	34		46		46					
Sr	74	99	61	9	72	24	22	35	40	53	82	81	96	52	227	123	27	58	106			
Zr	574	585	550	430	351	424	355	206	359		157		270	243	271			319	524			
Nb		59	57	101	62	69		24			23		42	53	18			64	32			
Hf	15	15			12	17	13		13	11	6.1	10	5.7		8.3		13					
Ta	1.4	5.0			5.4	4.7	8.7		1.2	4.3	2.4	5.1	1.9				5.8					
La	240	108	118	78	123	140	132	137	210	189	28.9	131	74.1	85.1	112	104.2	118	115	270			
Ce	440	202	129	60	247	246	241	197	380	350	55	235	152	170	193	137	217	156	327			
Nd	165	82			105	85	90		140	141	18	84	65		70		79					
Sm	26.7	14.1			21.0	13.2	15.1		22.5	22.8	2.7	13.5	13.9		10.2		13.5					
Eu	1.67	1.79			1.56	0.65	0.98		1.38	1.56	1.31	1.44	1.02		1.67		0.70					
Tb	2.7	1.7			3.9	2.2	2.8		2.5	2.9	0.5	2.0	1.0		0.7		2.3					
Yb	10.3	8.42	9.00	6.44	14.9	8.84	12.4	4.70	8.93	11.1	4.47	10.4	7.23	11.5	0.82	4.33	15.5	10.4	4.48			
Lu	1.53	1.33			2.22	1.35	2.02		1.27	1.64	0.77	1.70	1.20		0.10		2.41					
Y	92.2	70.9	80.0	62.2	108.0	57.0	90.0	46.7	54.8	103.8	31.4	75.0	76.0	83.1	13.8	60.3	116.8	83.5	36.3			
U	5.5	5.5			4.7	13.0	7.0		4.5	6.7	12.5	10.2	5.6		3.1		9.1					
Be	2.4	7.2	4.4	3.6	7.4	5.5	10.9	2.5	2.6	4.9	4.8	10.6		5.2	3.1	2.0	5.7	5.7	0.3			

Table 9:

Table 9
Major and trace element analyses of pink PPG and other granites of the potassic series, Pikes Peak batholith

	Quartz monzonite; Tarryall	Granite; Lake George	Granite, Redskin stock	Pink PPG			
Sample No.	86TQM[a]	86LG7	85RS2	GM-7-BG	WP-33-BG	85BP4	SPD1R
SiO_2	63.9	74.6	72.5	70.41	73.13	71.6	72.5
TiO_2	0.81	0.21	0.17	0.52	0.30	0.27	0.27
Al_2O_3	15.4	12.0	13.1	13.79	12.63	12.7	12.6
Fe_2O_3	1.21	0.66	0.93	3.75	3.18	0.65	0.58
FeO	4.52	1.44	1.82			2.79	2.41
MnO	0.13	0.03	0.03	0.08	0.08	0.07	0.06
MgO	0.63	0.14	0.1	0.55	0.14	0.11	0.12
CaO	3.50	0.81	0.94	1.57	1.03	1.14	0.98
Na_2O	3.55	2.94	3.67	3.37	3.21	3.24	3.19
K_2O	4.33	5.56	5.24	5.35	5.55	5.62	5.58
P_2O_5	0.31	0.02	0.02	0.19	0.03	0.02	0.02
Sum	98.29	98.41	98.52	99.58	99.28	98.21	98.31
Mg No.	16.7	10.9	6.3	22.5	8.0	5.5	6.8
Ni				5	6		
Cr				0.2	0.3		
V				10.0	2.6		
Sc				10.0	6.1		
Co				3.8	1.3		
Zn				80	100		
Ga							
Cs				1.5	2.3		
Ba	2800	310	270	1208	529	450	450
Rb	116	251	450	210	210	225	209
Th	10	41	69	32	30	34	32
Sr	440	51	23	173	67	47	55
Zr				557			
Nb	36	4	18			20	23
Hf				14	17		
Ta				3.8	3.5		
La	79	140		114	172	200	180
Ce	150	270		216	323	370	340
Nd	80.5	114.3		90	135	152.8	156.4
Sm	15.8	20.6		15.8	23.6	26.3	28
Eu				2.30	1.29		
Tb				2.1	3.1		
Yb	7	8	16	8.74	10.2	10	7
Lu				1.31	1.48		
Y	66	72	110	71.6	92.2	94	69
U				3.3	3.3		
Be				3.4	3.9		

[a] Although this sample was taken from the Tarryall sodic pluton (cf Fig. 1), it exhibits geochemical characteristics similar to potassic series granitoids. Thus it is included with that series here, in Table 11 and on all subsequent geochemical plots.

Table 10:

Table 10
Major and trace element analyses of gray monzogranites of the potassic series, Pikes Peak batholith

Sample No.	GM-8-JS	GM-19-JS	D-22-JS	GM-30-JS	WB-42-JS	GM-6-JS	P-26-JS	P-2-JS	GM-23-JS
SiO_2	64.76	64.53	69.10	69.89	68.26	64.20	64.20	67.27	68.47
TiO_2	1.13	1.08	0.57	0.24	0.71	1.13	1.02	0.83	0.61
Al_2O_3	14.20	13.57	14.81	13.99	13.69	13.97	13.57	13.96	13.93
Fe_2O_3	6.30	6.08	3.29	2.68	4.21	6.32	6.04	5.17	3.71
FeO									
MnO	0.13	0.12	0.07	0.07	0.09	0.12	0.13	0.11	0.09
MgO	1.08	1.04	0.56	0.43	0.68	1.08	1.04	0.81	0.57
CaO	3.51	3.35	1.56	1.48	2.25	3.46	3.16	2.67	1.96
Na_2O	3.38	3.12	3.43	3.57	3.27	3.24	3.23	3.31	3.27
K_2O	4.14	4.34	5.39	5.70	4.54	4.60	4.40	4.93	5.37
P_2O_5	0.56	0.46	0.22	0.06	0.25	0.52	0.55	0.40	0.25
Sum	99.17	97.68	99.00	98.11	97.95	98.62	97.33	99.46	98.22
Mg No.	25.3	25.2	25.3	24.0	24.3	25.2	25.4	23.7	23.4
Ni	3	7	6	11	7	6	5	7	5
Cr	12.2	15.7	10.7	13.7	13.0	9.9	9.4	8.7	9.1
V	52.8	66.8	14.9	12.2	34.2	51.2	52.4	42.2	15.2
Sc	14.3	13.2		6.7	11.7	12.9	13.4	12.2	10.7
Co	6.8	7.8	1.6		3.7	6.7	6.7	4.5	1.6
Zn	107	88		80	89	120	140	110	100
Ga	24	23		21	23	30	31		
Cs						1.3	1.4	1.4	2.3
Ba	1480	1546	1450	1064	1412	1568	1792	1498	1356
Rb						130	150	170	200
Th						10	13	23	24
Sr	305	327	194	179	212	307	325	278	198
Zr	536	505	399	346	458	528	556	528	448
Nb	40	30		21	27	35	38		
Hf						15	15	13	13
Ta						2.2	2.0	2.4	3.3
La	75.4	78.9	110	127	79.2	84.0	86.1	115	86.9
Ce	141	139	205	217	140	175	176	218	176
Nd						82	81	90	78
Sm						16.5	16.6	15.5	15.3
Eu						3.17	3.19	2.75	2.64
Tb						2.2	2.2	1.7	1.9
Yb	6.62	5.85	8.09	5.16	4.85	7.08	6.87	6.95	8.81
Lu						1.04	1.02	1.08	1.33
Y	69.8	58.7	71.2	52.1	53.5	63.8	63.3	68.2	84.4
U						2.7	2.6	3.4	3.0
Be	2.7	2.1	4.1	2.9		1.8	2.4	3.3	4.1

Table 11:

Table 11
Sm–Nd data for Pikes Peak samples [values for CHUR (Chondritic uniform reservoir) are $^{143}Nd/^{144}Nd = 0.512638$, $^{147}Sm/^{144}Nd = 0.1967$; Sm decay constant = 6.54 E−12 year^{-1})

Sample	Rock type	Sm (ppm)[a]	Nd (ppm)[a]	$^{147}Sm/^{144}Nd$ rock at present[b]	$^{143}Nd/^{144}Nd$ rock at present[b]	$^{143}Nd/^{144}Nd$ rock at 1.08 Ga	ϵ_{Nd} (T)[c]
Late-stage mafic rocks							
CCN-19B-CD	Gabbro	11.7	52.6	0.13445	0.512216	0.511263	+0.4
CCN-10-CD	Gabbro	7.8	40.2	0.11797	0.511925	0.511089	−3.0
LG-12-JD	Gabbro	16.3	81.5	0.12085	0.512162	0.511305	+1.2
86LG6	Gabbro	14.9	74.9	0.11994	0.512138	0.511288	+0.9
86TARG	Gabbro	9.2	43.7	0.12642	0.512143	0.511247	+0.1
MBC-8-SG	Mafic dike	9.6	42.6	0.13601	0.512388	0.511424	+3.5
S71PPG29	Mafic dike	9.6	42.8	0.13581	0.512383	0.511420	+3.5
Late-stage intermediate to felsic rocks, sodic series:							
S71PPG2A	Intermediate dike	40.1	208.3	0.11621	0.512054	0.511230	−3.0
S71PPG21	Intermediate dike	22.9	112.6	0.12268	0.512115	0.511245	0.0
GM-12-RB	Syenite	14.1	81.1	0.10538	0.512102	0.511355	+2.2
GM-35-RB	Syenite	29.6	199.1	0.08993	0.511965	0.511328	+1.6
86LG5	Syenite	11.0	61.1	0.10904	0.512024	0.511251	+0.1
LG-10-JD	Quartz syenite	25.5	160.6	0.09582	0.511953	0.511274	+0.6
MBC-7-BS	Fayalite granite	26.8	137.4	0.11784	0.512117	0.511281	+0.7
MBC-20-BS	Fayalite granite	21.8	97.2	0.13540	0.512168	0.511208	−0.7
MBC-6-BS	Fayalite granite	22.0	117.0	0.11340	0.512042	0.511238	−0.1
B65DSR	Fayalite granite	22.0	123.6	0.10758	0.512008	0.511245	0.0
B65F	Fayalite granite	23.6	107.4	0.13243	0.512177	0.511238	−0.1
86LG4	Fayalite granite	16.7	107.9	0.09314	0.511927	0.511267	+0.5
MBC-9-GK	Sodic amph. granite	21.6	106.8	0.12213	0.512125	0.511259	+0.3
85MR1	Sodic amph. granite	28.9	159.1	0.10968	0.512014	0.511237	−0.1
85TG1	Sodic amph. + bio. granite	35.7	199.8	0.10796	0.512008	0.511243	0.0
85AM1	Biotite granite	24.9	137.8	0.10904	0.511997	0.511224	−0.4
Late-stage felsic rocks, potassic series:							
PP-31-BG	Windy Point Granite	13.6	77.9	0.10564	0.511921	0.511172	−1.4
86LG7	Granite, Lake George	18.8	105.5	0.10774	0.511870	0.511106	−2.7
85RS2	Granite, Redskin stock	17.0	92.8	0.11073	0.512020	0.511235	−0.2
86TQM	Quartz Monzonite	15.2	76.9	0.11902	0.511962	0.511118	−2.5
Pikes Peak granite:							
GM-6-JS	Gray monzogranite	17.4	88.5	0.11872	0.511978	0.511136	−2.1
P-26-JS	Gray monzogranite	19.1	99.3	0.11646	0.512037	0.511212	−0.6
85BP4	Pink PPG	26.3	152.8	0.10399	0.511930	0.511193	−1.0
SPD1R	Pink PPG	20.5	115.1	0.10778	0.511990	0.511226	−0.3
87PP1	Pink PPG	14.3	78.2	0.11058	0.511915	0.511131	−2.2

[a] Sm and Nd concentrations determined by isotope dilution by addition of a mixed ^{149}Sm–^{150}Nd spike prior to sample dissolution.
[b] Repeated analysis of BCR-1 yielded $^{143}Nd/^{144}Nd = 0.512633$. Nd isotopic compositions were corrected for mass fractionation by normalizing to $^{146}Nd/^{144}Nd = 0.72190$.
[c] $\epsilon_{Nd}(T) = [(^{143}Nd/^{144}Nd(T)\text{sample}/^{143}Nd/^{144}Nd(T)_{CHUR}) - 1] \times 10000$, where T is the age of 1.08 Ga and $^{143}Nd/^{144}Nd(T)_{CHUR} = 0.511244$.

Figure 2:

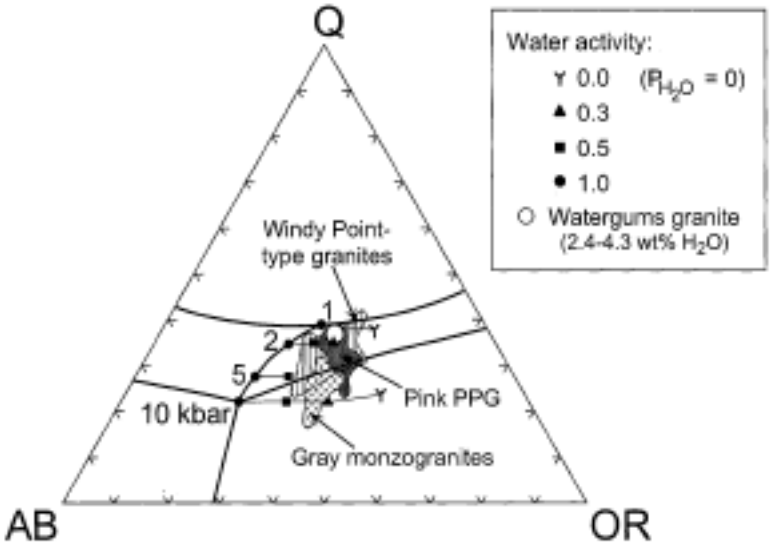

Fig. 2. Normative quartz–albite–orthoclase ternary diagram illustrating granite minima for different water activities (Ebadi and Johannes, 1991). Data for the Watergums granite are from Clemens et al. (1986). Data for the pink PPG are from Table 9 and Barker et al. (Table IV, 1975); other data are from Tables 8–10.

Figure 3:

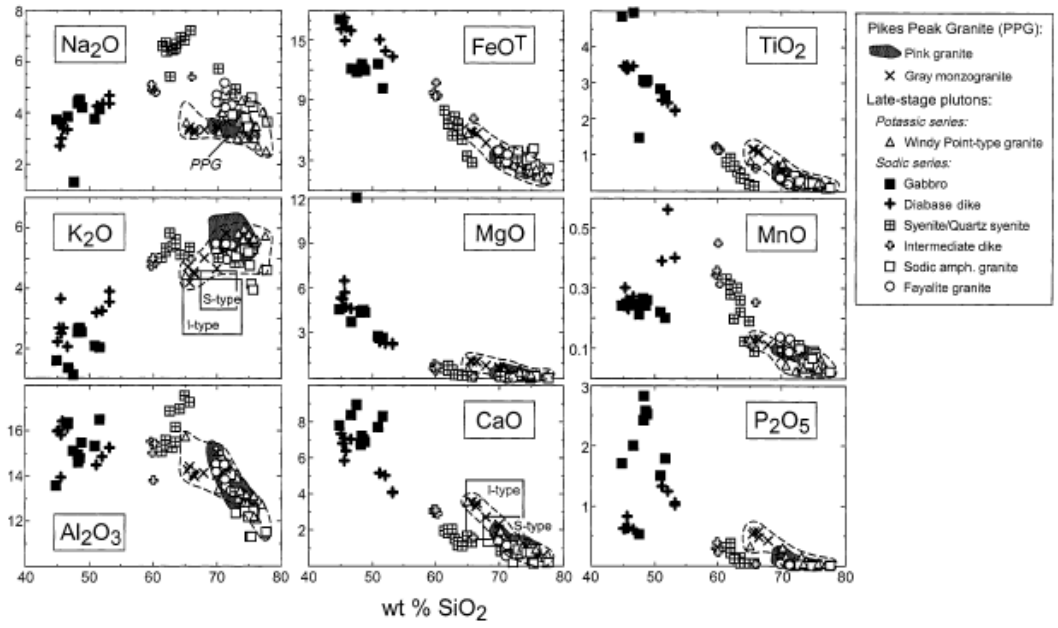

Fig. 3. Harker diagrams for Pikes Peak rocks. $FeO^T = (0.9 \times Fe_2O_3) + FeO$, and major element data were normalized to 100% on an anhydrous basis prior to plotting. Shaded fields for the pink PPG include data from Table 9 and from Barker et al. (1975). See legend for symbols. A dashed line has been drawn around samples of the potassic series analyzed here (Tables 8–10). Ranges in K_2O and CaO for S- and I-type granites are from Whalen et al. (1987).

Figure 4:

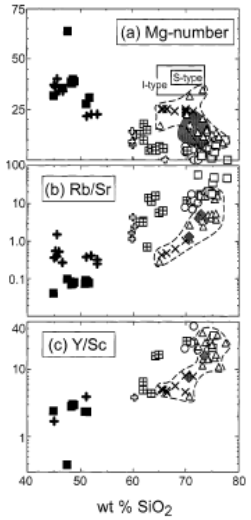

Fig. 4. (a) Mg-number ($100 \times$ molar Mg/[Mg+ Fe]), (b) log Rb/Sr and (c) log Y/Sc versus wt% silica in Pikes Peak samples. Symbols as in Fig. 3. In (a), the shaded field represents the PPG (data from Barker et al., 1975). In (b) and (c), shaded diamonds represent the pink PPG (data from Table 9, this study). Ranges in Mg-number for I- and S-type granites are from Whalen et al. (1987). The dashed lines encircle samples of the potassic series analyzed here (Tables 8–10).

Figure 5:

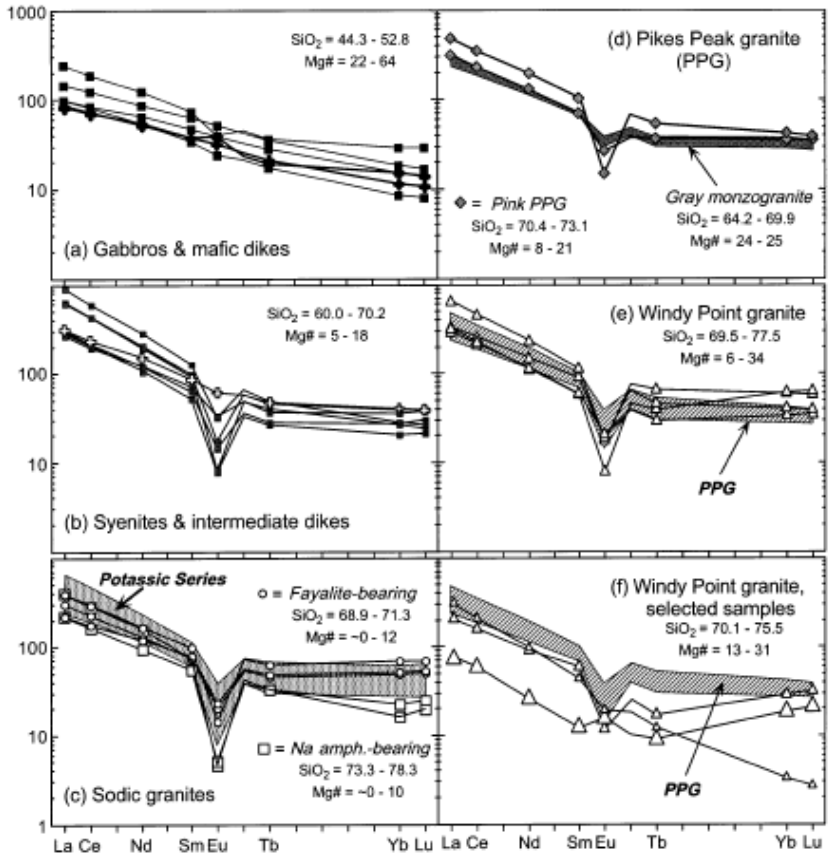

Fig. 5. Chondrite-normalized rare earth profiles for Pikes Peak rocks: (a) gabbros and diabase dikes, (b) syenites and intermediate dikes and (c) fayalite- and sodic amphibole-bearing granites, (d) gray monzogranite and pink PPG, (e) samples of Windy Point-type granite that exhibit 'typical' REE patterns and (f) selected samples of Windy Point-type granite that illustrate anomalous patterns compared to other Windy Point samples. Symbols as in Figs. 3 and 4. In (c), a field representing most Pikes Peak potassic granites [cf (d)–(f)] is shown for comparison. In (e) and (f), the ruled fields represent the gray monzogranites plus pink PPG.

Figure 6:

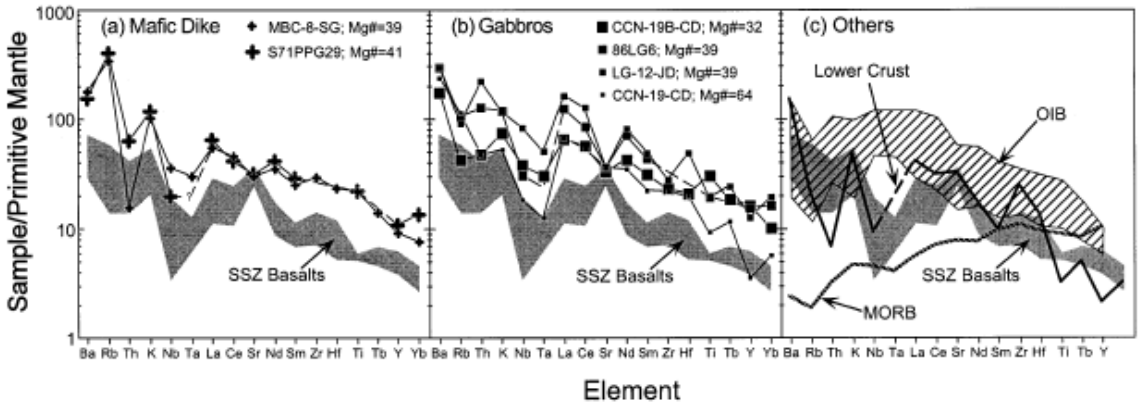

Fig. 6. Primitive mantle-normalized trace element diagrams for (a) two samples from a mafic dike from Mount Rosa, (b) gabbros of the Pikes Peak batholith and (c) other rock types [normalizing values from Taylor and McClennan (1985)]. The shaded fields in all panels represent typical subduction-related basalts [from Wilson (1989)]. Ranges for ocean island basalt [OIB; Weaver (1991)], estimates for lower crust (Weaver and Tarney, 1984), and average N-type MORB (Saunders and Tarney, 1984; Sun, 1980) are shown in (c).

Figure 7:

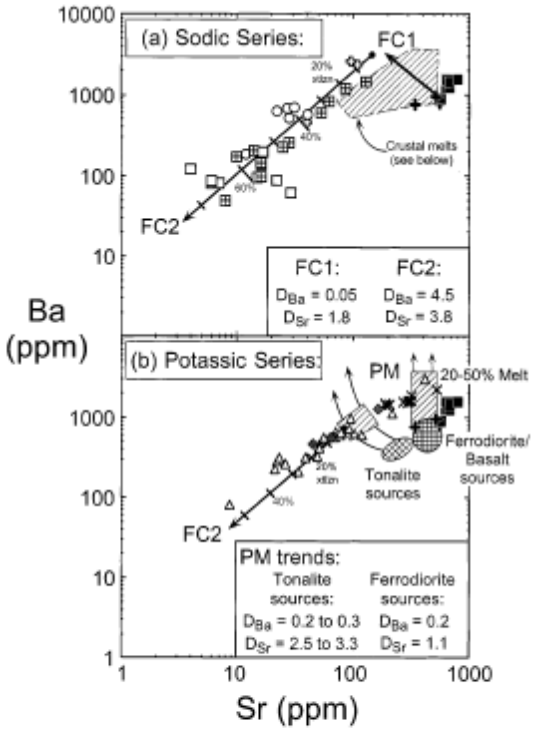

Fig. 7. Log Ba versus log Sr in Pikes Peak (a) sodic and (b) potassic series granitoid rocks (symbols as in Figs. 3 and 4). Pikes Peak mafic rocks are also plotted in both panels. Straight arrows labeled FC1 and FC2 represent trends for Rayleigh FC. The arrow labeled FC1 has a length that corresponds to 70% crystallization, and uses bulk partition coefficients (*D* values) appropriate for mafic compositions. The second fractionation trend, shown by the arrows labeled FC2 in (a) and (b), uses *D* values appropriate for evolved compositions, and tick marks representing increments of 10% crystallization are shown. The trends and depletions in Ba and Sr in many of the sodic granites and syenites (a) seemingly require extensive degrees of fractionation. In (b), curves are shown that represent trends for batch partial melting (PM) of selected crustal lithologies. The mean and median compositions of hundreds of analyses for post-Archean tonalitic rocks of granulite facies terrains were assumed for tonalite source compositions (Rudnick and Presper, 1990). Representative ferrodiorite compositions from Mitchell et al. (1996) were also assumed as sources. Ba and Sr contents in the ferrodiorites are similar to those in a mean composition of hundreds of analyses for granulite facies mafic xenoliths (Rudnick and Presper, 1990). Diagonally ruled fields on the PM curves represent 20–50% melting; a diagonally ruled field encompassing those compositions is also shown in (a).

Figure 8:

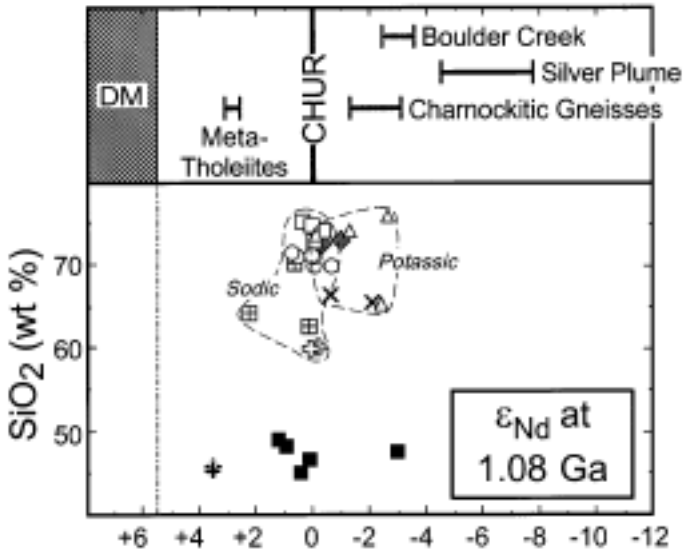

Fig. 8. ϵ_{Nd} at 1.08 Ga versus SiO_2 (wt%) for samples of the Pikes Peak batholith (Table 11) and associated wall rocks (DePaolo, 1981a). An additional $\epsilon_{Nd}(T)$ value of ~0 for the Silver Plume intrusions was omitted for clarity. Symbols as in Figs. 3 and 4.

Figure 9:

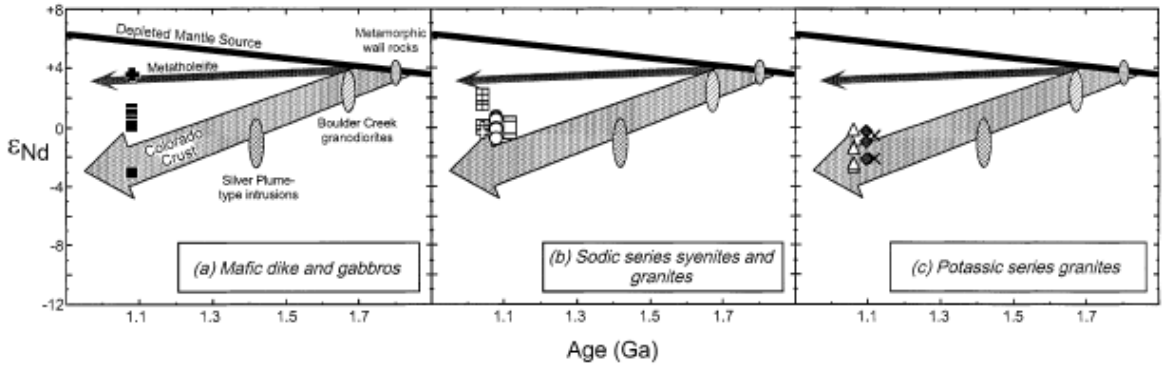

Fig. 9. ϵ_{Nd} versus age relationships for (a) mafic dike and gabbros, (b) sodic series syenites and granites and (c) potassic series granites of the Pikes Peak batholith. The large arrow and black line show ϵ_{Nd} evolution for typical 1.8 Ga Colorado crust and depleted mantle, respectively (from DePaolo, 1981a). The small arrow gives the ϵ_{Nd} evolution for typical 1.8 Ga metatholeiitic basalt, and fields are shown for metamorphic wall rocks, Boulder Creek granodiorites and Silver Plume-type intrusions (from DePaolo, 1981a). In (b) and (c), data points are separated for clarity and no age differences are implied. Symbols as in Figs. 3 and 4.

Figure 10:

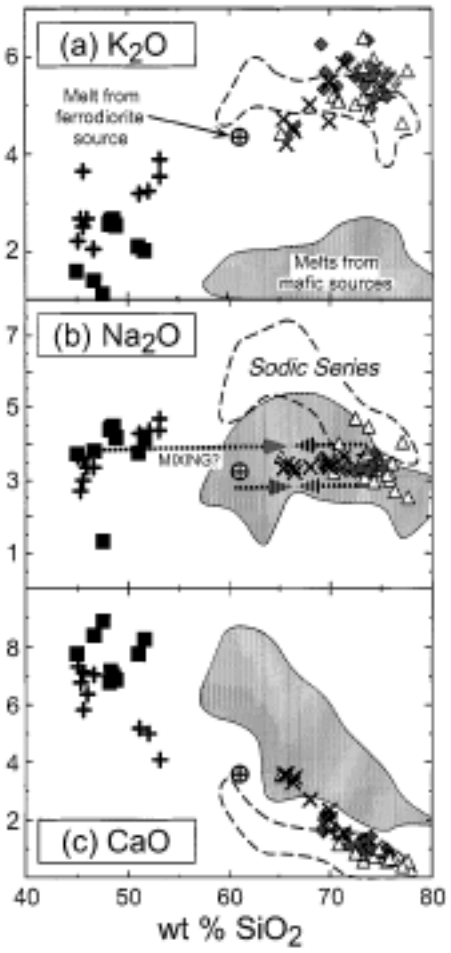

Fig. 10. (a) K_2O, (b) Na_2O and (c) CaO versus SiO_2 in Pikes Peak potassic granitoids and mafic rocks [symbols as in Figs. 3 and 4; data from this study and Barker et al. (1975)]. Dashed lines encircle compositions of Pikes Peak sodic granitoids. Shaded fields include compositions of melts generated from mafic source rocks; data from Holloway and Burnham (1972), Helz (1976), Spulber and Rutherford (1983), Rushmer (1991) and Beard and Lofgren (1991). Also shown is a melt composition (cross in circle) generated from a ferrodiorite source (Scoates et al., 1996).

Figure 11:

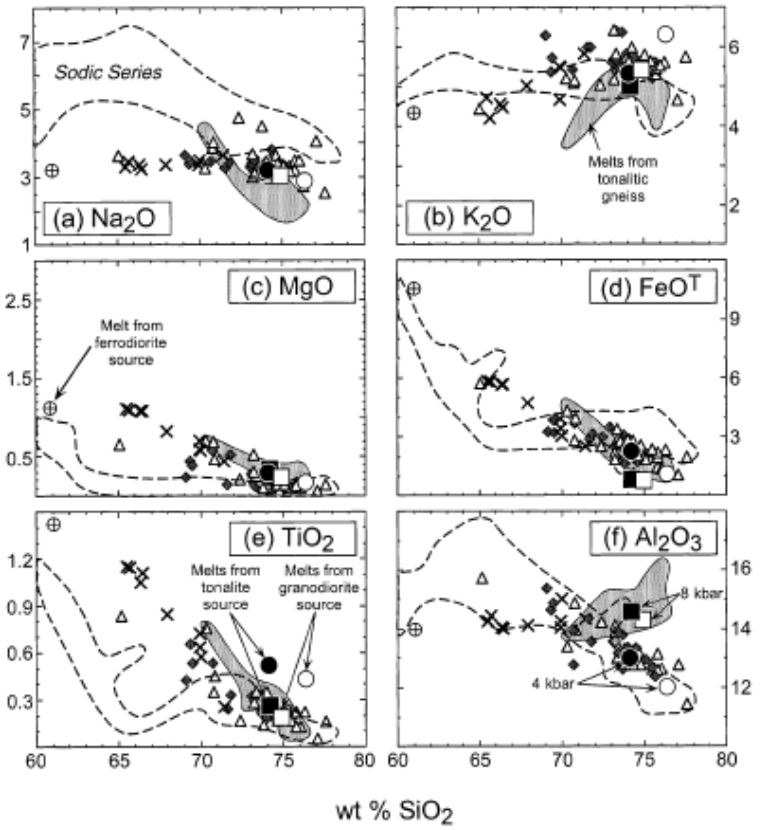

Fig. 11. Selected Harker diagrams illustrating rocks of the Pikes Peak potassic series. Individual data points (from Table 9 and Barker et al., 1975) for the pink PPG are shown by shaded diamonds; other symbols as in Fig. 3. Dashed lines encircle compositions of the Pikes Peak sodic series (cf Fig. 3). Shaded fields represent melts produced in experiments involving fluid-absent melting of tonalitic gneiss (Skjerlie and Johnston, 1993). Compositions of melts generated by partial melting of granodiorite and tonalite sources (from Patiño Douce, 1997) are shown by the following symbols: ○, granodiorite source at 4 kbar; □, granodiorite source at 8 kbar; ●, tonalite source at 4 kbar; ■, tonalite source at 8 kbar. Also shown is a melt composition (symbol = cross in circle) generated from a ferrodiorite source (Scoates et al., 1996).

Figure 12:

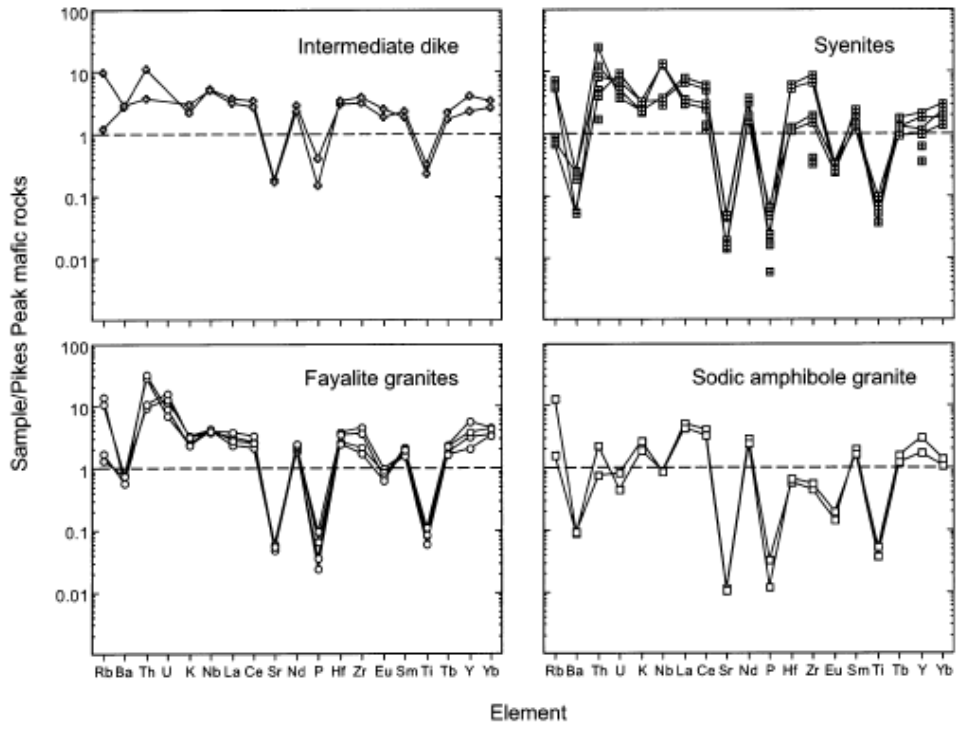

Fig. 12. Representative compositions of Pikes Peak sodic rocks normalized to representative Pikes Peak mafic rocks (gabbro sample CCN-19B-CD and diabase dike sample MBC-8-SG). Note the depletions in Ba, Sr, P, Eu and Ti, but enrichments in incompatible elements.

Figure 13:

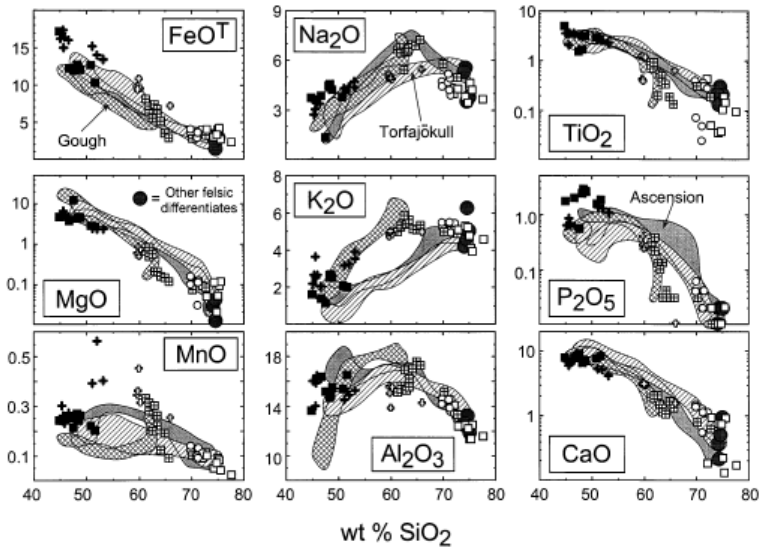

Fig. 13. Major element variations in Pikes Peak sodic rocks and ocean island suites. Symbols as in Fig. 3. Data sources for the ocean island suites as follows: Ascension Island (shaded field), Harris (1983); Torfajökull volcanic complex, Iceland (ruled field), Macdonald et al. (1990); Gough Island (checkerboard field), LeRoex (1985). Also illustrated are compositions of granites (large, filled circles) thought to represent fractionation products from coeval mafic rocks [data from Table 2 in Turner et al. (1992)]. Note that log scales are used for MgO, TiO_2, P_2O_5 and CaO.

Figure 14:

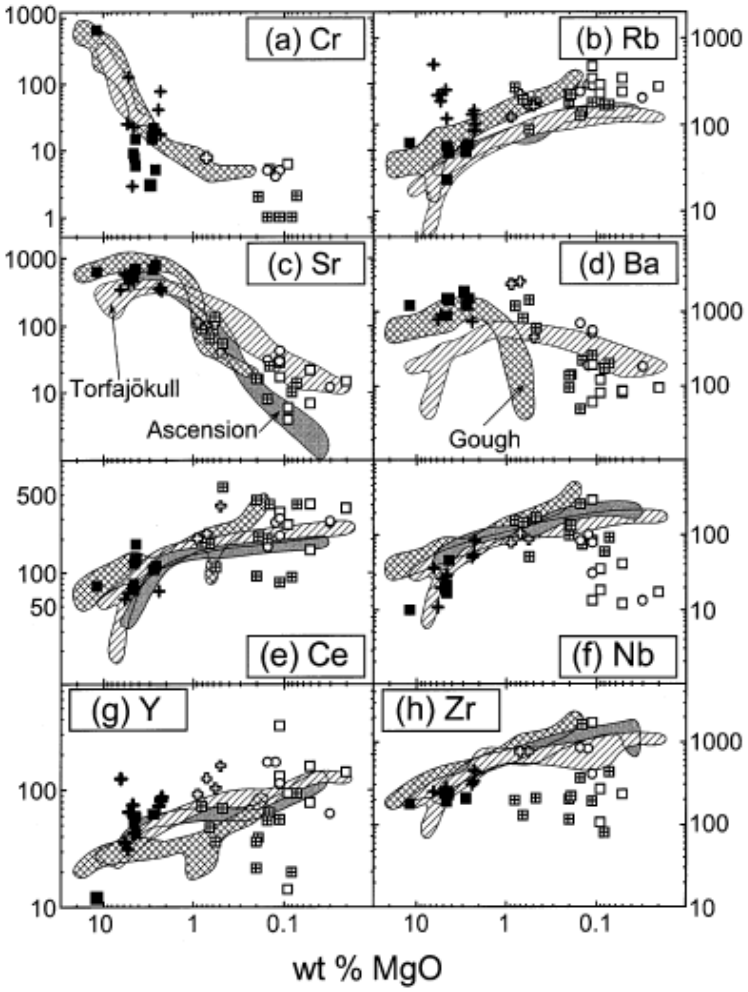

Fig. 14. Log–log plots of (a) Cr, (b) Rb, (c) Sr, (d) Ba, (e) Ce, (f) Nb, (g) Y and (h) Zr (ppm) versus MgO (wt%) in Pikes Peak sodic series rocks and selected ocean island suites. Symbols as in Fig. 3, and data sources and fields as in Fig. 13.

Figure 15:

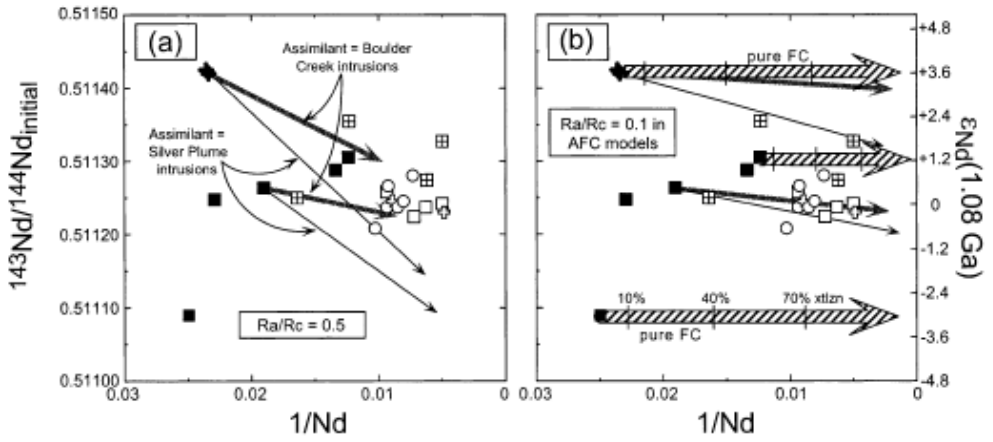

Fig. 15. Initial $^{143}Nd/^{144}Nd$ [or $\epsilon_{Nd}(1.08\ Ga)$] versus 1/Nd (ppm) for Pikes Peak sodic series rocks. Data are from Table 11 and symbols as in Fig. 3. Model trends for pure FC are shown in (b) as heavy ruled lines. Tick marks correspond to 10, 40 and 70% crystallization. Models trends for assimilation plus FC (AFC) processes [after DePaolo (1981b)] are illustrated in both panels. Assumed parental magmas include an average of two mafic dike samples and gabbro sample CCN-19B-CD. The bulk distribution coefficient for Nd assumed in both pure FC and AFC models is 0.13. In both panels, AFC trends that involve ~1.7 Ga Boulder Creek and ~1.4 Ga Silver Plume intrusions as assimilants are shown by heavy and fine lines, respectively. Average Nd concentrations and initial $^{143}Nd/^{144}Nd$ ratios for the assimilants were estimated from data given by DePaolo (1981a). In (a), the rate of assimilation versus crystallization (Ra/Rc) is 0.5; for AFC trends shown in (b), $R_a/R_c = 0.1$. The length of all arrows for AFC and pure FC trends corresponds to 95% crystallization (for the closed system equivalent). Even these extreme degrees of fractionation cannot produce the Nd concentrations in most sodic granitoids when $R_a/R_c = 0.5$ (a).